Comput Geosci (2012) 16:1101–1124
DOI 10.1007/s10596-012-9306-2

ORIGINAL PAPER

Numerical modeling of two-phase binary fluid mixing using mixed finite elements

Shuyu Sun · Abbas Firoozabadi · Jisheng Kou

Received: 1 April 2011 / Accepted: 27 June 2012 / Published online: 27 July 2012

Abstract Diffusion coefficients of dense gases in liquids can be measured by considering two-phase binary nonequilibrium fluid mixing in a closed cell with a fixed volume. This process is based on convection and diffusion in each phase. Numerical simulation of the mixing often requires accurate algorithms. In this paper, we design two efficient numerical methods for simulating the mixing of two-phase binary fluids in one-dimensional, highly permeable media. Mathematical model for isothermal compositional two-phase flow in porous media is established based on Darcy's law, material balance, local thermodynamic equilibrium for the phases, and diffusion across the phases. The time-lag and operator-splitting techniques are used to decompose each convection–diffusion equation into two steps: diffusion step and convection step. The Mixed finite element (MFE) method is used for diffusion equation because it can achieve a high-order and stable approximation of both the scalar variable and the diffusive fluxes across grid–cell interfaces. We employ the characteristic finite element method with moving mesh to track the liquid–gas interface. Based on the above schemes, we propose two methods: single-domain and two-domain methods. The main difference between two methods is that the two-domain method utilizes the assumption of sharp interface between two fluid phases, while the single-domain method allows fractional saturation level. Two-domain method treats the gas domain and the liquid domain separately. Because liquid–gas interface moves with time, the two-domain method needs work with a moving mesh. On the other hand, the single-domain method allows the use of a fixed mesh. We derive the formulas to compute the diffusive flux for MFE in both methods. The single-domain method is extended to multiple dimensions. Numerical results indicate that both methods can accurately describe the evolution of the pressure and liquid level.

Keywords Two-phase flow · Binary mixing · Multicomponent transport · Mixed finite element methods · Conservation law

S. Sun (✉) · J. Kou
Computational Transport Phenomena Laboratory,
Division of Physical Science and Engineering,
King Abdullah University of Science and Technology,
Thuwal 23955-6900, Kingdom of Saudi Arabia
e-mail: shuyu.sun@kaust.edu.sa

S. Sun · A. Firoozabadi
Reservoir Engineering Research Institute,
Palo Alto, CA, USA

A. Firoozabadi
Chemical and Environmental Engineering Department,
Mason Laboratory, Yale University,
New Haven, CT 06520, USA

J. Kou
School of Mathematics and Statistics, Hubei Engineering
University, Xiaogan 432100, Hubei, China

1 Introduction

Numerical modeling for single-phase and two-phase flow in porous media has wide applications in hydrology and petroleum reservoir engineering. Many investigators have focused on incompressible and immiscible flow in porous media, for example [4, 6–8, 16, 22, 23, 32–34]. Recently, two-phase nonequilibrium fluid mixing is attracting more attention because of its applications in a large number of problems. For example, in the

petroleum industry, gas is injected into oil reservoirs to maintain the reservoir pressure [15]. Once a substantial amount of the injected gas dissolves in the oil phase, fluid and surface properties, such as density, viscosity, and surface tension, may change significantly. This may cause the oil phase to flow faster through the reservoir, and the production is increased [13, 14].

Multicomponent mixtures are often treated as pseudobinaries in the petroleum literature [18, 30, 35, 36] studying the mixing occurring when hydrocarbon liquids are exposed to gases, such as methane and carbon dioxide. To describe the mixing process accurately, we require diffusion coefficients. However, conventional methods to measure diffusion coefficients can not be used at high pressures and temperatures [14]. The PVT cell technique [18, 28–30] is currently an attractive and powerful alternative for measuring high-pressure diffusion coefficients. This technique allows two nonequilibrium fluid phases to interact inside a closed cell at the constant temperature. In the approach used in [30], the cell with a fixed volume is closed; that is, no gas and liquid is injected or extracted at the boundaries of the cell. Thus, the total mass and volume in the cell are kept constant, but the mass transfer occurs across the interface of two fluid phases and inside each phase. The pressure and liquid volume will change with time which can be used to infer diffusion coefficients.

A numerical model has been developed in [14] to describe nonequilibrium mass transport between the gas and liquid phases of a binary mixture in a closed PVT cell of fixed volume. In this paper, we consider the case of porous media that are encountered in the petroleum industry. Mathematical model for isothermal compositional two-phase flow in porous media will be obtained by Darcy's law, material balance, thermodynamic equilibrium between the phases, and diffusion within and between phases. This model incorporates diffusion and dispersion (within bulk phases) into compositional two-phase flow in porous media, and we consider scenarios where diffusion and dispersion are significant. Although our model itself can apply to multiple dimensions, for simplification, we focus on the one-dimensional, highly permeable porous media in this paper.

Operator splitting technique [1, 9, 11, 20, 24, 32] is widely used to reduce the original complex time-dependent physical problem into simpler problems based on the time-lag of dimension or physics. The IMplicit–EXplicit method [2, 3, 12, 17, 21] treats some terms implicitly and evaluates the others explicitly, and as a result, it is more stable than the fully explicit scheme and can convert the original equations into an implementation-friendly form. Mathematical model describing two-phase compositional flow in porous media is a time-dependent and nonlinear system of partial differential equations. In order to design efficient algorithm, we first apply the time-lag and operator-splitting techniques to decompose each convection–diffusion equation into two steps: diffusion step and convection step. We apply an explicit temporal scheme for the diffusion step, while in convection step, we treat the molar density of each phase implicitly, but with explicit treatment for other variables.

We propose two different methods: single-domain and two-domain. In the two-domain approach, we make assumption that the liquid and the gas have a distinct interface. This assumption often happens in the case of two-phase flow in one-dimensional, highly permeable media without capillarity. Different from two-domain method, the single-domain method removes this assumption to simulate two-phase flow with the saturation between 0 and 1. Moreover, it can be readily extended to multidimensional domain. We use the characteristic finite element method with moving mesh (for the two-domain method) or with fixed mesh (for the single-domain method) to track the convection, and employ the mixed finite element (MFE) method for the diffusion equation. The characteristic finite element method alleviates the Courant number restriction and can use reasonably large time steps, along with producing nonoscillatory solutions without numerical diffusion. The MFE method approximates simultaneously the scalar variable (the mole fraction of component) and the diffusive fluxes across the numerical block interfaces and can achieve a high-order and stable approximation of both variables.

The article is organized as the following. In Section 2, we propose mathematical model for isothermal compositional two-phase flow in porous media with molecular diffusion and mechanical dispersion. In Section 3, a two-domain method is developed to solve the system of a binary fluid in one-dimensional, highly permeable media. In Section 4, we propose a single-domain method to solve the two-phase convection–diffusion process in one-dimensional, highly permeable media and extend it to two dimensional domain. In Section 5, we provide two numerical examples to demonstrate the efficiency of our methods. Finally, we draw conclusions.

2 Mathematical model

Modeling equations for isothermal compositional two-phase flow in porous media consist of (1) Darcy's law for phase velocities in the two phases, (2) transport

equations for each species, and (3) local thermodynamic equilibrium at the interface between the phases.

Species transport equations In the past, the governing equations modeling transport of multicomponents in single-phase flow have been outlined in the literature, such as [5]. In this paper, we propose the expression of transport equations for two-phase compositional flow. The equations that model the transport of species are obtained from the material balance of each species:

$$\phi\frac{\partial\,(cz_i)}{\partial t}+\nabla\cdot\left(F_{\mathrm{conv},i}+F_{\mathrm{diff},i}\right)=q_i,\quad i=1,2,\cdots,n_c,$$

$$F_{\mathrm{conv},i}=\sum_{\alpha=L,G}c_\alpha x_{i,\alpha}\mathbf{u}_\alpha,$$

$$F_{\mathrm{diff},i}=-\sum_{\alpha=L,G}S_\alpha c_\alpha D_{i,\alpha}\nabla x_{i,\alpha}.$$

Here, we denote porosity by ϕ and the overall molar density by c. We use α as the phase index, and i as the component or species index; n_c is the total number of components in the system. z_i is the overall mole fraction of component i; $x_{i,\alpha}$ is the mole fraction of component i in phase α; and c_α is the molar density of phase α. q_i is the source term, which can be used to represent well flux. The bulk flow causes the convection of species; the convection flux $F_{\mathrm{conv},i}$ is summation of convection flux of component i in both phases. The molecular diffusion and mechanical dispersion together are modeled by the diffusion–dispersion flux $F_{\mathrm{diff},i}$. In this paper, however, we neglect mechanical dispersion and focus only on molecular diffusion. The linear relation between the diffusion flux $F_{\mathrm{diff},i}$ and the gradient of mole fraction above is known as Fick's law.

Darcy's law The phase flux/velocity ($\mathbf{u}_\alpha$) is given by Darcy's law for multiphase flow:

$$\mathbf{u}_\alpha=-\frac{k_{r\alpha}}{\mu_\alpha}\mathbf{K}\left(\nabla p-\rho_\alpha\mathbf{g}\right),\quad \alpha=L,G,$$

where K is the absolute permeability of the porous medium; $k_{r\alpha}$, μ_α, and ρ_α are the relative permeability, viscosity, and mass density of phase α, respectively; and p denotes the pressure and $\mathbf{g}$ the gravitational vector. We have neglected capillarity in this work. Relative permeabilities are functions of saturations.

Fluid properties and phase equilibrium calculations The phase and volumetric behaviors (including the calculations of the fugacities) are modeled by using the Peng–Robinson equation of state [27]. Viscosity of oil and gas phases is a function of temperature, pressure, and phase composition, and it is estimated based on the methodology of Lohrentz et al. [25].

Binary fluid in 1-D highly permeable media In the rest of this paper, we first restrict our attention to a binary fluid in a one-dimensional, highly permeable medium, and at the end of Section 4, we will consider multiple dimensional cases. We also assume zero source term $q_i=0$. The transport equation and Darcy's law are now simplified to the following system over $x\in\Omega=[0,H]$, $t\in[0,T_f]$:

$$\phi\frac{\partial\,(cz_i)}{\partial t}+\frac{\partial}{\partial x}\times\left(\sum_{\alpha=L,G}c_\alpha x_{i,\alpha}u_\alpha-\sum_{\alpha=L,G}S_\alpha c_\alpha D_{i,\alpha}\frac{\partial x_{i,\alpha}}{\partial x}\right)=0,\quad i=1,2,\tag{2.1}$$

$$u_\alpha+\frac{k_{r\alpha}K}{\mu_\alpha}\frac{\partial p}{\partial x}=0,\quad \alpha=L,G.\tag{2.2}$$

All boundaries are considered impermeable, and both Darcy velocity u_α and diffusive fluxes must vanish at the boundaries:

$$u_\alpha=0,\quad x\in\partial\Omega=\{0,H\},\ \alpha=L,G,$$

$$c_\alpha D_{i,\alpha}\nabla x_{i,\alpha}=0,\quad x\in\partial\Omega=\{0,H\},\ i=1,2,\ \alpha=L,G.$$

Initial conditions are imposed for the overall molar density by c and the overall mole fraction z_i:

$$c(x,t)=c_{\mathrm{init}}(x),\quad t=0,$$

$$z_i(x,t)=z_{i,\mathrm{init}}(x),\quad t=0.$$

Additional simplification can be made by taking the advantage that the permeability K is sufficiently large. Noting that the Darcy velocity is a finite number, and the relative permeability and viscosity are all bounded, but K is sufficiently large (infinity), we then conclude that

$$\frac{\partial p}{\partial x}\approx 0,$$

or the pressure p is a constant with respect to the spatial direction (varies as time changes). This fact will be used below to design fast algorithm for this system.

We note that similar results can be obtained for the fluid flow in open space. In this case, for example, the flow is described by Navier–Stokes equations. As a result, the system of a binary fluid in one-dimensional, highly permeable media can be also used to model the nonequilibrium mass transport between the gas and liquid phases of a binary mixture in a closed PVT cell of fixed volume.

3 Two-domain mixed finite element method

In the section, we propose a two-domain method for solving the system of a binary fluid in one-dimensional, highly permeable media. We make assumption that the liquid and the gas have a distinct interface; that is, we assume that the saturation $S_L = 1 - S_G$ has the value of either one or zero, but not between. We note that without capillarity, two-phase flow in one-dimensional, highly permeable media often results in clear interface between two phases. This assumption allows us to define two domains: the gas region and the liquid region.

$$\Omega_L := \{x \in \Omega : \ S_L(x,t) = 1\},$$

$$\Omega_G := \{x \in \Omega : \ S_G(x,t) = 1\}.$$

Clearly, Ω_L and Ω_G vary with time and $\Omega = \Omega_L \cup \Omega_G$. We assume $\Omega_L = (0, H_I)$ and $\Omega_G = (H_I, H)$, where $H_I = H_I(t)$ is the location of liquid–gas interface.

Within the liquid region Ω_L, the species transport equation becomes as follows:

$$\phi \frac{\partial \left(c_L x_{i,L}\right)}{\partial t} + \frac{\partial}{\partial x}\left(c_L x_{i,L} u_L - c_L D_{i,L} \frac{\partial}{\partial x} x_{i,L}\right) = 0, \quad i = 1, 2.$$

Similarly, within the gas region Ω_G, the species transport equation becomes

$$\phi \frac{\partial \left(c_G x_{i,G}\right)}{\partial t} + \frac{\partial}{\partial x}\left(c_G x_{i,G} u_G - c_G D_{i,G} \frac{\partial}{\partial x} x_{i,G}\right) = 0, \quad i = 1, 2.$$

We first apply time splitting to decompose the above convection–diffusion equation into two steps: diffusion step and convection step. In diffusion step, we solve

$$\frac{\phi\left(c_L^k x_{i,L}^{k+1/2} - c_L^k x_{i,L}^k\right)}{t_{k+1} - t_k} - \frac{\partial}{\partial x}\left(c_L^k D_{i,L}^k \frac{\partial}{\partial x} x_{i,L}^m\right) = 0, \quad i = 1, 2,$$

where the superscripts k, $k+1/2$, and m indicate the corresponding time steps; m can be chosen to be $m = k+1/2$ for implicit time stepping (backward Euler scheme for time integration), or $m = k$ for explicit time stepping (forward Euler scheme for time integration). For a binary system, $x_{1,L}^k = 1 - x_{2,L}^k$, so we need consider only the first component in the simulation:

$$\frac{\phi\left(c_L^k x_{1,L}^{k+1/2} - c_L^k x_{1,L}^k\right)}{t_{k+1} - t_k} - \frac{\partial}{\partial x}\left(c_L^k D_{1,L}^k \frac{\partial}{\partial x} x_{1,L}^m\right) = 0. \tag{3.1}$$

Exactly the same approach can be applied for the gas region, so we will not repeat it here and below.

In convection step, we solve

$$\frac{\phi\left(c_L^{k+1} x_{1,L}^{k+1} - c_L^{k+1/2} x_{1,L}^{k+1/2}\right)}{t_{k+1} - t_k} - \frac{\partial}{\partial x}\left(c_L^{k+1} x_{1,L}^{k+1/2} u_L^{k+1/2}\right) = 0, \tag{3.2}$$

$$u_L^{k+1} + \frac{k_{rL}^{k+1/2} K}{\mu_L^{k+1/2}} \frac{\partial p^{k+1}}{\partial x} = 0. \tag{3.3}$$

Again, the same approach can be applied for the gas region, which is skipped here for brevity.

Diffusion step In this step, we attempt to solve Eq. 3.1 using mixed finite element method. We first rewrite Eq. 3.1 in a weak formulation: to seek for $x_{1,L}^{k+1/2} \in W \coloneqq L^2(\Omega_L)$ and $F_{\text{diff}} \in V \coloneqq H_0(\text{div}, \Omega_L) = \left\{v \in L^2(\Omega) : \frac{dv}{dx} \in L^2(\Omega) \text{ and } v|_{x=0} = 0\right\}$ such that the following two equations hold:

$$\left(\frac{\phi\left(c_L^k x_{1,L}^{k+1/2} - c_L^k x_{1,L}^k\right)}{t_{k+1} - t_k}, w\right) + \sum_E \left(F_{\text{diff}}, w \cdot \mathbf{n}\right)_{\partial E} - \sum_E \left(F_{\text{diff}}, \frac{dw}{dx}\right)_E = 0, \ \forall w \in W,$$

$$\left(\left(c_L^k D_{1,L}^k\right)^{-1} F_{\text{diff}}, v\right) + \left(x_{1,L}^m, v \cdot \mathbf{n}\right)_{\partial\Omega} - \sum_E \left(x_{1,L}^m, \frac{dv}{dx}\right)_E = 0, \ \forall v \in V.$$

Here, E represents the element, which is a subinterval in one dimension.

For finite dimensional approximation, we apply the lowest-order Raviart–Thomas space (RT_0). Let $0 = X_0^k < X_1^k < X_2^k < \cdots < X_n^k = H_I(t_k) < X_{n+1}^k < \cdots < X_{N-1}^k < h_N^k = H$ be the mesh at the time step k. Let $W_h \subset L^2(\Omega)$ be the piecewise-constant space and let $V_h \subset H_0(\text{div}, \Omega)$ be the conforming (thus continuous)

piecewise linear space. The mixed finite element formulation becomes as follows: to seek for $x_{1,L}^{k+1/2} \in W := W_h$ and $F_{\text{diff}} \in V_h$ such that the following two equations hold:

$$\left(\frac{\phi\left(c_L^k x_{1,L}^{k+1/2} - c_L^k x_{1,L}^k\right)}{t_{k+1} - t_k}, w\right) + \sum_E \left(F_{\text{diff}}, w\cdot\mathbf{n}\right)_{\partial E} = 0, \ \forall w \in W_h, \tag{3.4}$$

$$\left(\left(c_L^k D_{1,L}^k\right)^{-1} F_{\text{diff}}, v\right) + \left(x_{1,L}^m, v\cdot\mathbf{n}\right)_{\partial\Omega} - \sum_E \left(x_{1,L}^m, \frac{dv}{dx}\right)_E = 0, \ \forall v \in V_h. \tag{3.5}$$

To reduce notation complexity, we denote the mixed finite element solution and the exact weak solution above using the same symbol set. Since w is constant within each element, the term involving its derivative vanishes in Eq. 3.4. If we choose explicit time stepping (i.e., $m = k$), then Eq. 3.5 decouples from Eq. 3.4; that is, we can calculate the diffusive flux first, then substitute it into Eq. 3.4 to compute the mole fraction $x_{1,L}^{k+1/2}$. If we integrate the first term in Eq. 3.5 exactly, this equation is still a system of simultaneous equations for all velocities on element interfaces. We can also apply trapezoid quadrature rule for the first term in Eq. 3.5 to decouple the system and to get explicit formulas for each individual diffusive flux.

Mass transfer between two domains The above diffusion step is performed for each domain (liquid or gas region) individually. We still need to specify a right boundary condition (or a top boundary condition for a vertical domain) at $x = H_I$ for the diffusion in liquid region and a left boundary condition (or a bottom boundary condition for a vertical domain) at $x = H_I$ for the diffusion in gas region. We assume that at the gas–liquid interface, the composition is in two-phase equilibrium. In a binary system, the composition at the interface between two phases is uniquely determined by thermodynamic equilibrium; that is, interfacial composition is only a function of temperature and pressure. We denote the equilibrium composition by $x_{i,L}^*$ and $x_{i,G}^*$. First, let us consider Fickian diffusion alone across the gas–liquid interface from the liquid side at time step $(k+1)$:

$$J_{i,L}^{k+1} = -c_L^{k+1,n} D_L^{k+1,n} \frac{x_{i,L}^* - x_{i,L}^{k+1,n}}{\left(h_n^{k+1}/2\right)}, \quad i = 1, 2.$$

Similarly, Fickian diffusion across the gas–liquid interface from the gas side at time step $(k+1)$ is

$$J_{i,G}^{k+1} = -c_G^{k+1,n+1} D_G^{k+1,n+1} \frac{x_{i,G}^{k+1,n+1} - x_{i,G}^*}{\left(h_{n+1}^{k+1}/2\right)}, \quad i = 1, 2.$$

In the above equations, the superscripts $k+1$ and n indicate the time step and spatial point index, respectively.

Since in the convection step, our mesh follows the movement of gas–liquid interface, we account for the bulk flow between gas–liquid interface in the diffusion step through the boundary condition on F_{diff}. The mass balance across the gas–liquid interface (considering the bulk flow across the interface) has the following form:

$$F_{i,L-G} = J_{i,L}^{k+1} + c_L^{k+1,n} x_{i,L}^* v_L = J_{i,G}^{k+1} + c_G^{k+1,n} x_{i,G}^* v_G, \quad i = 1, 2.$$

Summing this balance equation over the two components yields

$$c_L^{k+1,n} v_L = c_G^{k+1,n} v_G.$$

Consequently, we have

$$J_{i,L}^{k+1} - J_{i,G}^{k+1} = -c_G^{k+1,n} v_G \left(x_{i,L}^* - x_{i,G}^*\right) = -c_L^{k+1,n} v_L \left(x_{i,L}^* - x_{i,G}^*\right), \quad i = 1, 2.$$

We then conclude

$$F_{i,L-G} = J_{i,L}^{k+1} + c_L^{k+1,n} x_{i,L}^* v_L = J_{i,L}^{k+1} - \frac{J_{i,L}^{k+1} - J_{i,G}^{k+1}}{x_{i,L}^* - x_{i,G}^*} x_{i,L}^*,$$

which can be used to specify the boundary condition for F_{diff} for the diffusion computational step on the gas–liquid interface.

Convection step In this step, we solve the convection part Eqs. 3.2–3.3 by assuming the absolute permeability is sufficiently large. We can then assume that the pressure is constant in space (but varies with time). We use the characteristic finite element method with moving mesh to track the convection. Let $X_0^{k+1} < \cdots < X_n^{k+1} = H_I(t_{k+1}) < \cdots < X_N^{k+1}$ be the mesh at the time step $(k+1)$. We define the element size

$$h_i^k := X_i^k - X_{i-1}^k, \quad i = 1, 2, \cdots, N.$$

Let $c_L^{k,i}$, p^k and $x_{1,L}^{k,i}$ be the molar density of the liquid phase at time step k in element i. Similar notation applies to the gas phase. We note that p^k does not have a spatial subscript i because it is independent of the

space. We use the following equation system to determine p^{k+1}, h_i^{k+1}, $c_L^{k+1,i}$, $x_{1,L}^{k+1,i}$, $c_G^{k+1,i}$, and $x_{1,G}^{k+1,i}$:

$$x_{1,L}^{k+1,i} = x_{1,L}^{k,i}, \quad i = 1, 2, \cdots, n, \tag{3.6}$$

$$x_{1,G}^{k+1,i} = x_{1,G}^{k,i}, \quad i = n+1, n+2, \cdots, N, \tag{3.7}$$

$$h_i^{k+1} c_L^{k+1,i} = h_i^k c_L^{k,i}, \quad i = 1, 2, \cdots, n, \tag{3.8}$$

$$h_i^{k+1} c_G^{k+1,i} = h_i^k c_G^{k,i}, \quad i = n+1, n+2, \cdots, N, \tag{3.9}$$

$$c_L^{k+1,i} = c_L\left(x_{1,L}^{k+1,i}, p^{k+1}\right),$$

$$i = 1, 2, \cdots, n, \tag{3.10}$$

$$c_G^{k+1,i} = c_G\left(x_{1,G}^{k+1,i}, p^{k+1}\right),$$

$$i = n+1, n+2, \cdots, N, \tag{3.11}$$

$$\sum_{i=1}^{N} h_i^{k+1} = H = \sum_{i=1}^{N} h_i^k. \tag{3.12}$$

The total number of equations above is $(3N+1)$. We also have $(3N+1)$ unknowns: $x_{1,L}^{k+1,i}$ $(i = 1, 2, \cdots, n,)$, $x_{1,G}^{k+1,i}$ $(i = n+1, n+2, \cdots, N)$, h_i^{k+1} $(i = 1, 2, \cdots, N)$, $c_L^{k+1,i}$ $(i = 1, 2, \cdots, n,)$, $c_G^{k+1,i}$ $(i = n+1, n+2, \cdots, N)$, and p^{k+1}. All the other unknowns can be expressed as explicit functions of p^{k+1}, so the system can be reduced to a nonlinear equation of a single unknown, which can be efficiently solved by Newton's method.

We note that after the system undergoes convection, some elements reduce their sizes while other elements increase their sizes. This is problematic especially for the element right besides the liquid–gas interface, which might quickly reduce its size to zero, causing computational pause due to CFL condition time step limitation from diffusion step. A fix for this problem is to merge the smallest element to its neighboring element if its size is substantially smaller than its neighbor. To keep the number of elements constant, we also split the largest element into two whenever we merge two elements into one.

4 Single-domain mixed finite element method

The two-domain method introduced previously tracks the gas–liquid interface explicitly, and it thus can capture the interface sharply. However, this method is difficult to extend to multidimensional domain because it resolves the gas–liquid interface by a moving mesh approach. Moreover, for truly porous media two-phase flow with the saturation between 0 and 1, the previous two-domain method certainly does not apply. In this section, we introduce another method to solve the two-phase convection–diffusion process in one-dimensional, highly permeable media. We do not need to make assumption that the liquid and the gas have a clear interface; that is, the saturation $S_L = 1 - S_G$ could have any value between one and zero.

Instead of solving liquid-phase and gas-phase species transport equation separately, we solve the combined two-phase species transport Eq. 2.1. We again apply time splitting to decompose the convection–diffusion equation into two steps: diffusion step and convection step. We may consider only the first component in the simulation for a binary system.

In diffusion step, we solve

$$\frac{\phi\left(c^k z_1^{k+1/2} - c^k z_1^k\right)}{t_{k+1} - t_k} - \frac{\partial}{\partial x}\left(\sum_{\alpha=L,G} S_\alpha^k c_\alpha^k D_{1,\alpha}^k \frac{\partial}{\partial x} x_{1,\alpha}^k\right) = 0, \tag{4.1}$$

where the superscripts k, and $k+1/2$ indicate the corresponding time steps. We have chosen to use explicit time stepping for convenience. However, implicit time stepping can be formulated in a similar way.

In convection step, we solve

$$\frac{\phi\left(c^{k+1} z_1^{k+1} - c^{k+1/2} z_1^{k+1/2}\right)}{t_{k+1} - t_k} - \frac{\partial}{\partial x} \times \left(\sum_{\alpha=L,G} c_\alpha^{k+1} x_{1,\alpha}^{k+1/2} u_\alpha^{k+1/2}\right) = 0, \tag{4.2}$$

$$u_\alpha^{k+1} + \frac{k_{r\alpha}^{k+1/2} K}{\mu_\alpha^{k+1/2}} \frac{\partial p^{k+1}}{\partial x} = 0. \tag{4.3}$$

Diffusion step The diffusion Eq. 4.1 can be also written as follows:

$$\frac{\phi\left(c^k z_1^{k+1/2} - c^k z_1^k\right)}{t_{k+1} - t_k} + \frac{\partial F_{\text{diff}}}{\partial x} = 0,$$

$$F_{\text{diff}} + \sum_{\alpha=L,G} S_\alpha^k c_\alpha^k D_{1,\alpha}^k \frac{\partial x_{1,\alpha}^k}{\partial x} = 0.$$

We note that $S_\alpha, c_\alpha, D_{i,\alpha}$, and $x_{i,\alpha}$ can be calculated from the overall composition z_i and pressure p using local equilibrium. The weak formulation of Eq. 4.1 is to seek for $z_{1,L}^{k+1/2} \in W \coloneqq L^2(\Omega_L)$ and $F_{\text{diff}} \in V := H_0(\text{div}, \Omega_L) =$

$\left\{v \in L^2(\Omega):\ \frac{dv}{dx} \in L^2(\Omega) \text{ and } v|_{x=0} = 0\right\}$, such that the following two equations hold:

$$\left(\frac{\phi\left(c^k z_1^{k+1/2} - c^k z_1^k\right)}{t_{k+1} - t_k}, w\right) + \sum_E \left(F_{\text{diff}}, w \cdot \mathbf{n}\right)_{\partial E} - \sum_E \left(F_{\text{diff}}, \frac{dw}{dx}\right)_E = 0,\ \forall w \in W,$$

$$F_{\text{diff}} = S_L^k F_{L,\text{diff}} + S_G^k F_{G,\text{diff}},$$

$$\left(\left(c_\alpha^k D_{1,\alpha}^k\right)^{-1} F_{\alpha,\text{diff}}, v\right) + \left(x_{1,\alpha}^k, v \cdot \mathbf{n}\right)_{\partial\Omega} - \sum_E \left(x_{1,\alpha}^k, \frac{dv}{dx}\right)_E = 0,\ \forall v \in V,\ \alpha = 1, 2.$$

The mixed finite element scheme is just to replace W and V above by appropriate finite dimensional space such as the Raviart–Thomas space. This scheme works well in two-phase region, but it needs special treatment in singe-phase region. For example, $(c_L^k D_{1,L}^k)$ is not well defined in the gas single-phase region; however, $F_{L,\text{diff}}$ is not needed in this region as it multiplies by $S_L^k = 0$ to get the desired F_{diff}. Thus the number of equations need to be reduced properly in a single-phase region.

Hybrid mixed finite element method might be more convenient to apply in the current scenario. In hybrid mixed finite element scheme, we introduce the overall composition unknown $z_{1,L}^k$ on element interfaces. Considering a single element E, we can establish the hybrid mixed finite element scheme using the lowest-order Raviart–Thomas space:

$$\left(\frac{\phi\left(c^k z_1^{k+1/2} - c^k z_1^k\right)}{t_{k+1} - t_k}, w\right)_E + \sum_E \left(F_{\text{diff}}, w \cdot \mathbf{n}\right)_{\partial E} = 0,\ \forall w \in W_h,$$

$$F_{\text{diff}} = S_L^k F_{L,\text{diff}} + S_G^k F_{G,\text{diff}},$$

$$\left((c_\alpha^k D_{1,\alpha}^k)^{-1} F_{\alpha,\text{diff}}, v\right)_E + \left(x_{1,\alpha}^k, v \cdot \mathbf{n}\right)_{\partial E} - \sum_E \left(x_{1,\alpha}^k, \frac{dv}{dx}\right)_E = 0,\ \forall v \in V_h,\ \alpha = 1, 2.$$

For a binary system, we can make further simplification by noting that the individual phase composition in two-phase region is constant, and thus it must have zero Fickian diffusion in two-phase region. Without loss of generality, we consider the diffusive flux $F_{\text{diff}}^{\partial E}$ on the right-hand boundary of an element E. We use the original variables c_α^k, $D_{1,\alpha}^k$, $x_{1,\alpha}^k$, z_1^k etc. to denote the corresponding variables at the center of the element (or they could also be viewed as the averaged values over the element); and we denote the value on the right-hand boundary of the element by $c_\alpha^{k,\partial E}$, $D_{1,\alpha}^{k,\partial E}$, $x_{1,\alpha}^{k,\partial E}$, $z_1^{k,\partial E}$ etc. The size of the element E is denoted by h_E. The equilibrium composition at the interface of two phases is denoted by $x_{i,L}^*$ and $x_{i,G}^*$. To derive our formulas, we make an assumption that the diffusive flux is constant across the region from the element center to its right-hand boundary. Equivalently, we can employ the trapezoid quadrature rule to approximate the integral $\left((c_\alpha^k D_{1,\alpha}^k)^{-1} F_{\alpha,\text{diff}}, v\right)_E$, which leads to the following explicit formula to compute the diffusive flux:

$$F_{\alpha,\text{diff}} = -c_\alpha^k D_{1,\alpha}^k \frac{x_{1,\alpha}^{k,\partial E} - x_{1,\alpha}^k}{h_E/2}.$$

The formulas to compute the diffusive flux will be considered in the following cases. If $S_L^{k,\partial E} = 1$ and $S_L^k = 1$, then there exists only liquid phase in the element and its right-hand boundary, and thus we have the form as

$$F_{\text{diff}}^{\partial E} = -c_L^k D_{1,L}^k \frac{z_1^{k,\partial E} - z_1^k}{h_E/2}, \quad \text{if } S_L^{k,\partial E} = 1 \text{ and } S_L^k = 1.$$

Similarly,

$$F_{\text{diff}}^{\partial E} = -c_G^k D_{1,G}^k \frac{z_1^{k,\partial E} - z_1^k}{h_E/2}, \quad \text{if } S_L^{k,\partial E} = 0 \text{ and } S_L^k = 0.$$

If $S_L^{k,\partial E} \in (0, 1)$ and $S_L^k \in (0, 1)$, the individual phase composition in two-phase region is constant for a binary system; that is, $x_{1,\alpha}^{k,\partial E} = x_{1,\alpha}^k = x_{1,\alpha}^*$. Therefore, it must have zero Fickian diffusion:

$$F_{\text{diff}}^{\partial E} = 0, \quad \text{if } S_L^{k,\partial E} \in (0, 1) \text{ and } S_L^k \in (0, 1).$$

If $S_L^{k,\partial E} \in (0, 1)$ and $S_L^k = 1$, there exists only liquid phase in the element, but its right-hand boundary is the interface of two phases, so we have

$$F_{\text{diff}}^{\partial E} = -c_L^k D_{1,L}^k \frac{x_{1,L}^* - z_1^k}{h_E/2}, \quad \text{if } S_L^{k,\partial E} \in (0, 1) \text{ and } S_L^k = 1.$$

Similarly,

$$F_{\text{diff}}^{\partial E} = -c_G^k D_{1,G}^k \frac{x_{1,G}^* - z_1^k}{h_E/2}, \quad \text{if } S_L^{k,\partial E} \in (0, 1) \text{ and } S_L^k = 0,$$

$$F_{\text{diff}}^{\partial E} = -c_L^{k,\partial E} D_{1,L}^{k,\partial E} \frac{z_1^{k,\partial E} - x_{1,L}^*}{h_E/2}, \quad \text{if } S_L^{k,\partial E} = 1 \text{ and } S_L^k \in (0, 1),$$

$$F_{\text{diff}}^{\partial E} = -c_G^{k,\partial E} D_{1,G}^{k,\partial E} \frac{z_1^{k,\partial E} - x_{1,G}^*}{h_E/2},$$

$$\text{if } S_L^{k,\partial E} = 0 \text{ and } S_L^k \in (0,1).$$

If $S_L^{k,\partial E} = 1$ and $S_L^k = 0$, we need first to determine the interface of two fluid phases. Since the diffusive flux across a finite size of two-phase region must be zero in a binary system, there must exist a sharp liquid–gas interface (i.e., fine size of two-phase region does not exist) under the the assumption of constant diffusive flux within the half cell region. We use h_c to denote the distance from the element center to the liquid–gas interface. By the assumption that the diffusive flux is constant across the region from the element center to its right-hand boundary, we have

$$F_{\text{diff}}^{\partial E} = -c_L^{k,\partial E} D_{1,L}^{k,\partial E} \frac{z_1^{k,\partial E} - x_{1,L}^*}{h_E/2 - h_c} = -c_G^k D_{1,G}^k \frac{x_{1,G}^* - z_1^k}{h_c}.$$

We then obtain

$$h_c = \frac{h_E/2}{1 + c_L^{k,\partial E} D_{1,L}^{k,\partial E} \left(z_1^{k,\partial E} - x_{1,L}^*\right) / \left(c_G^k D_{1,G}^k \left(x_{1,G}^* - z_1^k\right)\right)}.$$

Consequently, the diffusive flux is expressed as follows:

$$F_{\text{diff}}^{\partial E} = -c_L^{k,\partial E} D_{1,L}^{k,\partial E} \frac{z_1^{k,\partial E} - x_{1,L}^*}{h_E/2} - c_G^k D_{1,G}^k \frac{x_{1,G}^* - z_1^k}{h_E/2},$$

$$\text{if } S_L^{k,\partial E} = 1 \text{ and } S_L^k = 0.$$

We can analogously derive

$$F_{\text{diff}}^{\partial E} = -c_G^{k,\partial E} D_{1,G}^{k,\partial E} \frac{z_1^{k,\partial E} - x_{1,G}^*}{h_E/2} - c_L^k D_{1,L}^k \frac{x_{1,L}^* - z_1^k}{h_E/2},$$

$$\text{if } S_L^{k,\partial E} = 0 \text{ and } S_L^k = 1.$$

We note that unlike the two-domain method in previous section, no special treatment is necessary for the mass transfer between the liquid region and the gas region because every element in this method can potentially hold liquid-phase, gas-phase, or two-phase mixture.

Convection step In this step, we solve the convection part Eqs. 4.2–4.3 by assuming the absolute permeability is sufficiently large. Like before, we assume that the pressure is constant in space (varies with time). We use the characteristic finite element method with moving mesh to track the convection. Using the same notation as we did in the previous section, we formulate the following equation system to determine p^{k+1}, $\widehat{h}_i$, $\widehat{c}^{k+1,i}$, and $\widehat{z}_1^{k+1,i}$:

$$\widehat{z}_{1,L}^{k+1,i} = z_{1,L}^{k,i}, \quad i = 1, 2, \cdots, N,$$

$$\widehat{h}_i \widehat{c}^{k+1,i} = h_i^k c^{k,i}, \quad i = 1, 2, \cdots, N,$$

$$\widehat{c}^{k+1,i} = c\left(\widehat{z}_1^{k+1,i}, p^{k+1}\right), \quad i = 1, 2, \cdots, N,$$

$$\sum_{i=1}^{N} \widehat{h}_i = H = \sum_{i=1}^{N} h_i.$$

The total number of equations above is $(3N + 1)$, which is the same as the number of unknowns. After elimination, the system can be reduced to a nonlinear equation of a single unknown (the pressure), which can be efficiently solved by Newton's method.

After obtaining $\widehat{c}^{k+1,i}$ and $\widehat{z}_1^{k+1,i}$ in the mesh formed by $\widehat{h}_i$ (let us call it $\widehat{\mathcal{E}}_h$), we project them back to the original mesh formed by h_i (let us call it $\mathcal{E}_h$):

$$\int_E c^{k+1,i} dx = \sum_{\widehat{E} \in \widehat{\mathcal{E}}_h} \int_{E \cap \widehat{E}} \widehat{c}^{k+1,i} dx, \quad \forall E \in \mathcal{E}_h,$$

$$\int_E c^{k+1,i} z_1^{k+1,i} dx = \sum_{\widehat{E} \in \widehat{\mathcal{E}}_h} \int_{E \cap \widehat{E}} \widehat{c}^{k+1,i} \widehat{z}_1^{k+1,i} dx, \quad \forall E \in \mathcal{E}_h.$$

The computed values $c^{k+1,i}$ and $z_1^{k+1,i}$ will be used for the calculation in the next time step while $\widehat{h}_i$ is discarded.

Extension to two dimensional domain The single-domain scheme can be conveniently extended to multiple spatial dimension since it uses a fixed mesh. The main difference between one-dimensional method and its multiple dimensional extension is to construct the approaches for computing the pressure and updating the mole fractions by convection. For simplification, we consider a two-dimensional domain with rectangular mesh. We assume that the mole fractions $z_i^{k+1/2}$ have been calculated by the diffusion equation similar to one-dimensional case. The pressure equation [37, 38] is described as

$$\begin{aligned}\phi c_f \frac{\partial p}{\partial t} &- (\overline{v}_1 - \overline{v}_2)\nabla \cdot (c_L x_{1,L} \lambda_L + c_G x_{1,G} \lambda_G)\mathbf{K}\nabla p \\ &- \overline{v}_2 \nabla \cdot (c_L \lambda_L + c_G \lambda_G)\mathbf{K}\nabla p = (\overline{v}_1 - \overline{v}_2)\nabla \\ &\cdot (c_L S_L D_L \nabla x_{1,L} + c_G S_G D_G \nabla x_{1,G}),\end{aligned}$$

Table 1 Relevant data for 1-D experiment

Parameters	Values
H	0.2194 m
T	310.95
K h_0	0.0768 m
P_0	10.2 MPa

Table 2 Component data used in the PR-EOS for 1-D experiment

	T_c (K)	P_c (MPa)	ω	s
C_1	190.6	4.54	0.008	−0.154
nC_5	469.7	3.37	0.251	−0.042

where $\lambda_\alpha = \frac{k_{r\alpha}}{\mu_\alpha}$, c_f is the total fluid compressibility, and $\overline{v}_i$ is the total partial molar volume of the ith component. The details of c_f and $\overline{v}_i$ is found in [10]. Using the lowest-order Raviart–Thomas space on a single element E, we can establish the hybrid mixed finite element scheme for pressure equation: for any $w \in W_h$, $v \in V_h$, such that

$$\left(\phi c_f^k \frac{p^{k+1}-p^k}{t_{k+1}-t_k}, w\right)_E + \left(\left(\overline{v}_1^k - \overline{v}_2^k\right)\nabla\cdot\mathbf{u}_a, w\right)_E + \left(\overline{v}_2^k \nabla\cdot\mathbf{u}_b, w\right)_E = \left(\left(\overline{v}_1^k - \overline{v}_2^k\right)\nabla\cdot\mathbf{F}, w\right)_E, \quad (4.4)$$

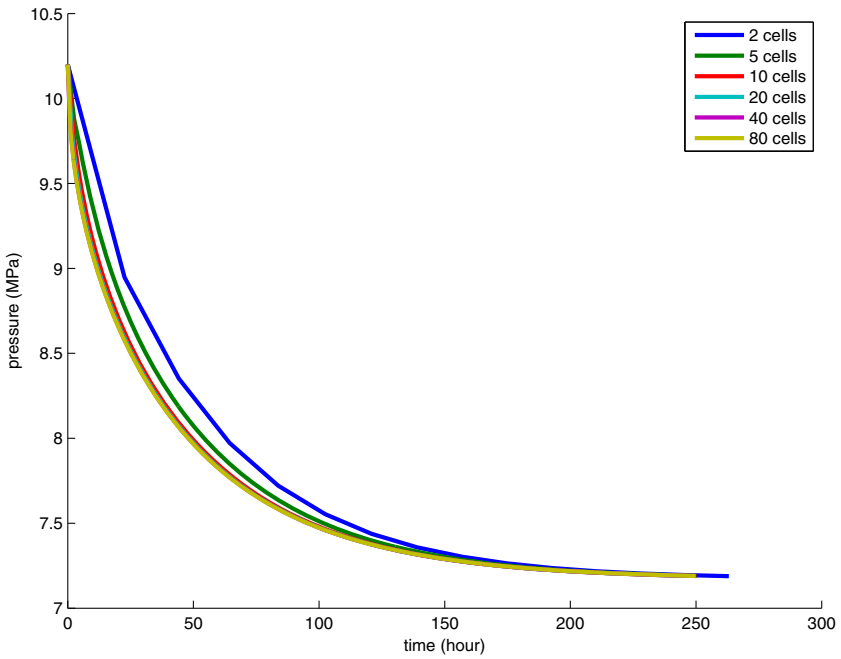

(a) Pressure as a function of time

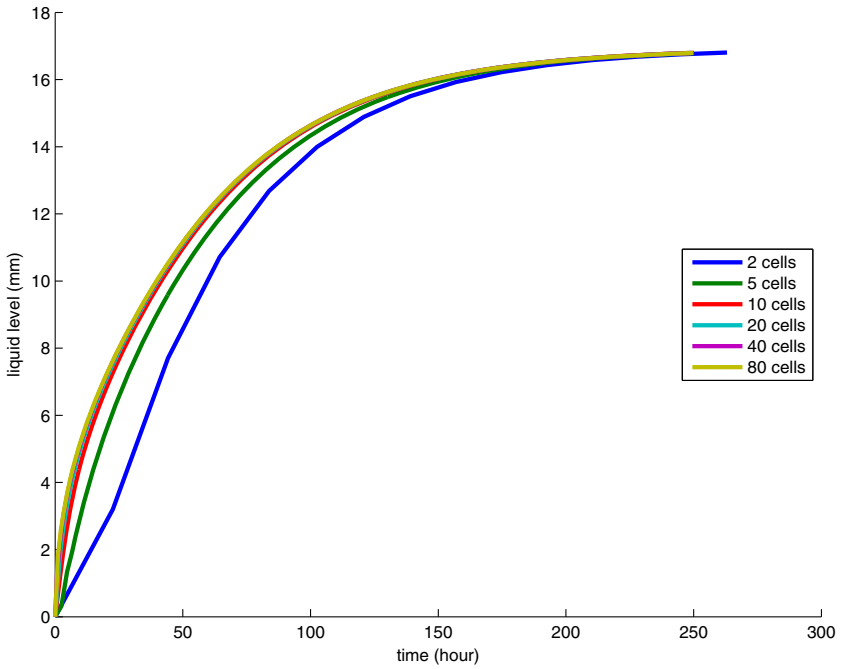

(b) Liquid level as a function of time

Fig. 1 Influence of the mesh on the simulated pressure and liquid level using the two-domain method

$$\left(\left(c_L^k x_{1,L}^k \lambda_L^k + c_G^k x_{1,G}^k \lambda_G^k\right)^{-1} \mathbf{K}^{-1}\mathbf{u}_a, v\right)_E = \left(p^{k+1}, \nabla \cdot v\right)_E - \left(p^{k+1}, v \cdot \mathbf{n}\right)_{\partial E}, \tag{4.5}$$

$$\left(\left(c_L^k \lambda_L^k + c_G^k \lambda_G^k\right)^{-1} \mathbf{K}^{-1}\mathbf{u}_b, v\right)_E = \left(p^{k+1}, \nabla \cdot v\right)_E - \left(p^{k+1}, v \cdot \mathbf{n}\right)_{\partial E}, \tag{4.6}$$

$$\mathbf{F} = \mathbf{F}_L + \mathbf{F}_G, \tag{4.7}$$

$$\left(\left(c_L^k S_L^k D_L\right)^{-1} \mathbf{F}_L, v\right)_E = \left(x_{1,L}^k, \nabla \cdot v\right)_E - \left(x_{1,L}^k, v \cdot \mathbf{n}\right)_{\partial E}, \tag{4.8}$$

$$\left(\left(c_G^k S_G^k D_G\right)^{-1} \mathbf{F}_G, v\right)_E = \left(x_{1,G}^k, \nabla \cdot v\right)_E - \left(x_{1,G}^k, v \cdot \mathbf{n}\right)_{\partial E}. \tag{4.9}$$

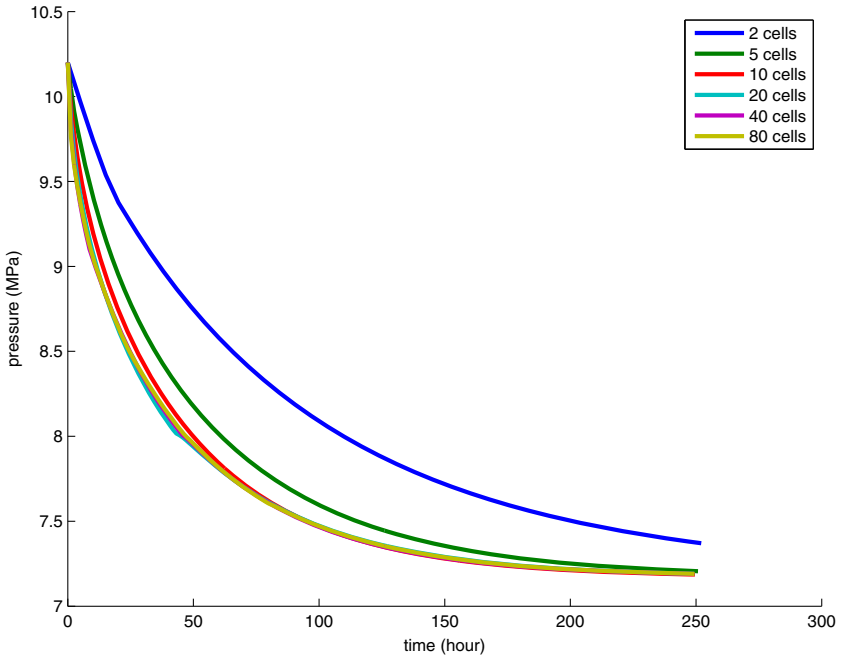

(a) Pressure as a function of time

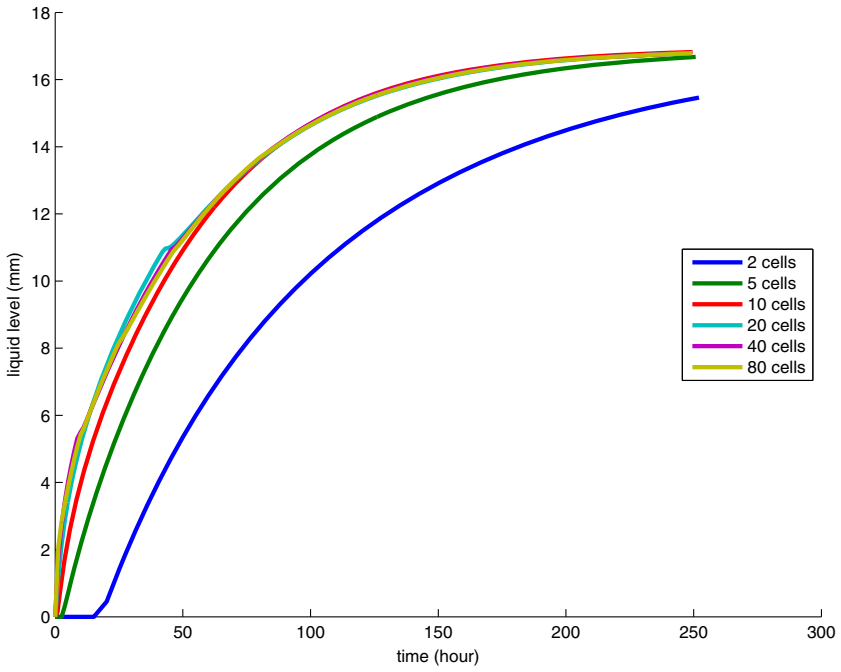

(b) Liquid level as a function of time

Fig. 2 Influence of the mesh on the simulated pressure and liquid level using the single-domain method

Similar to Eq. 3.5, we can also apply trapezoid quadrature rule for the first term of Eqs. 4.5, 4.6, 4.8, and 4.9 to decouple the system and to get explicit formulas for each individual flux. We use piecewise-constant approximation for the compositions, and then Eq. 4.4 becomes

$$\begin{aligned}\left(\phi c_f^k \frac{\partial p}{\partial t}, w\right)_E &+ \left(\overline{v}_1^k - \overline{v}_2^k\right)|_E \left(\mathbf{u}_a \cdot \mathbf{n}, w\right)_{\partial E} \\ &+ \overline{v}_2^k|_E \left(\mathbf{u}_b \cdot \mathbf{n}, w\right)_{\partial E} \\ &= \left(\overline{v}_1^k - \overline{v}_2^k\right)|_E \left(\mathbf{F} \cdot \mathbf{n}, w\right)_{\partial E}.\end{aligned}$$

As a result, we can obtain the discretization equation of pressure. After obtaining the pressure, we define the total molar flux [26] as

$$\mathbf{u}^{k+1} = -\left(c_L^k \lambda_L^k + c_G^k \lambda_G^k\right) \mathbf{K} \nabla p^{k+1}.$$

Let

$$f_i^k = \frac{c_L^k x_{i,L}^k \lambda_L^k + c_G^k x_{i,G}^k \lambda_G^k}{c_L^k \lambda_L^k + c_G^k \lambda_G^k}.$$

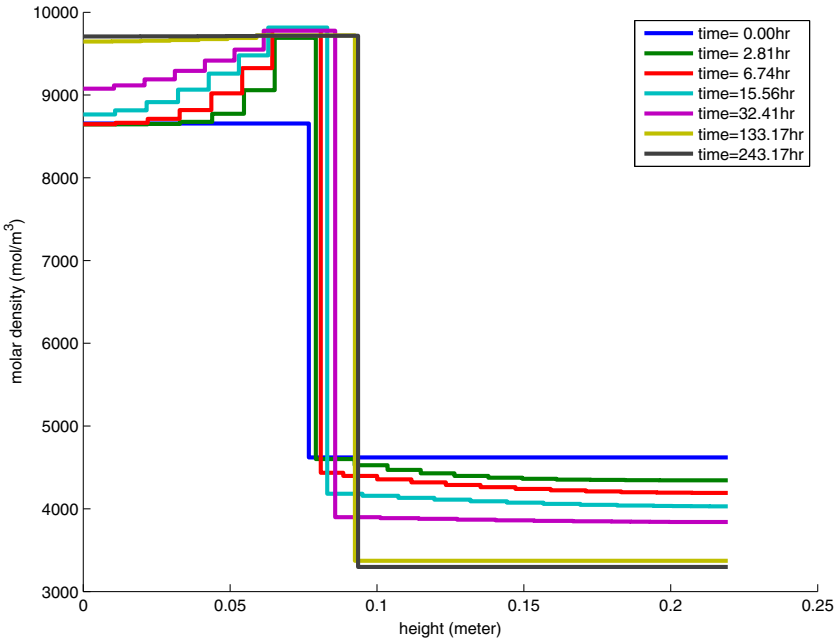

(a) Two-domain method

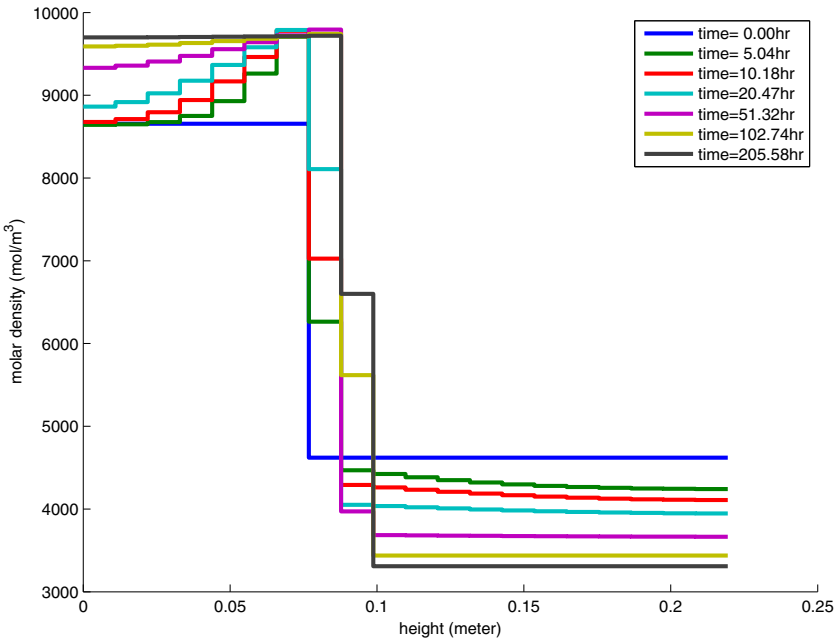

(b) Single-domain method

Fig. 3 Molar density simulated on a mesh of 20 cells

We now consider the convection equation to update z_i. Based on the operator splitting, the convection equation becomes

$$\phi \frac{c^k \left(z_i^{k+1} - z_i^{k+1/2} \right)}{t_{k+1} - t_k} + \mathbf{u}^{k+1} \cdot \nabla f_i^k = 0. \tag{4.10}$$

Integrating Eq. 4.10 over a single element E, we obtain

$$\int_E \phi \frac{c^k \left(z_i^{k+1} - z_i^{k+1/2} \right)}{t_{k+1} - t_k} + \int_E \mathbf{u}^{k+1} \cdot \nabla f_i^k = 0.$$

Green's theorem gives us

$$\int_E \mathbf{u}_L \cdot \nabla f_i = \int_{\partial E} \mathbf{u} \cdot \mathbf{n} f_i - \int_E f_i \nabla \cdot \mathbf{u}.$$

Let the elements E_γ^1 and E_γ^2 share the edge γ with $\mathbf{n}_\gamma$ exterior to E_γ^1; that is, $\gamma = E_\gamma^1 \bigcap E_\gamma^2$, then we define

$$f_i^*|_\gamma = \begin{cases} f_i|_{E_\gamma^1}, & \text{if } \mathbf{u} \cdot \mathbf{n}_\gamma \geq 0, \\ f_i|_{E_\gamma^2}, & \text{if } \mathbf{u} \cdot \mathbf{n}_\gamma < 0. \end{cases}$$

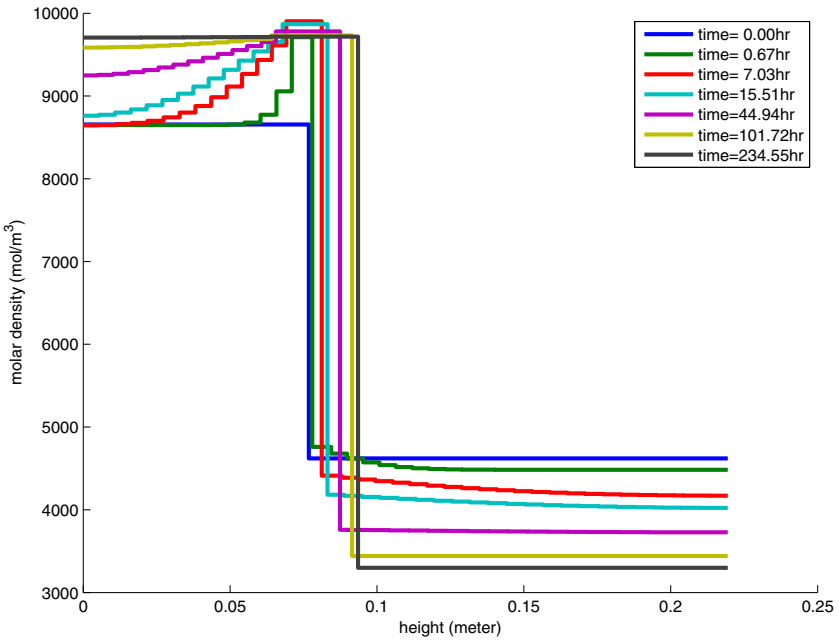

(a) Two-domain method

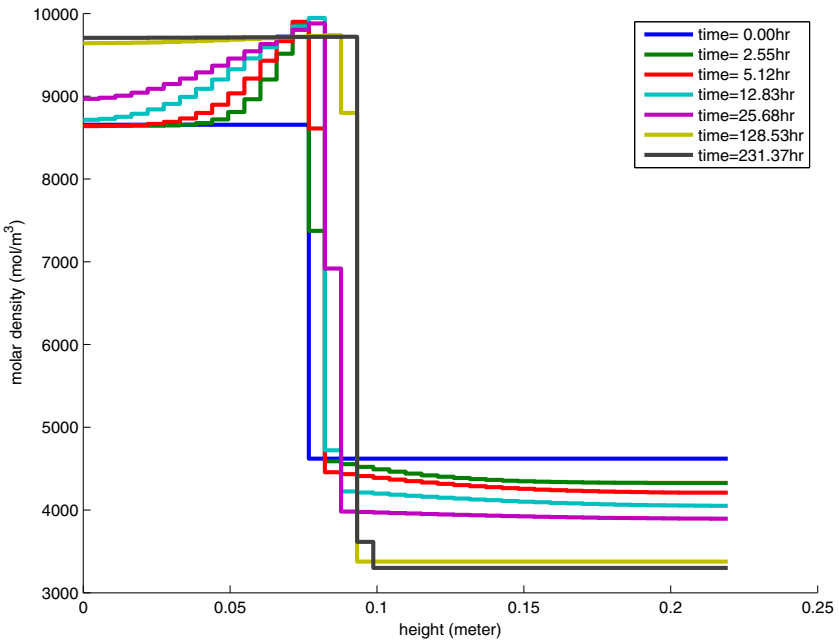

(b) Single-domain method

Fig. 4 Molar density simulated on a mesh of 40 cells

We take the upwind values of f_i on the edges ∂E of element E as

$$\int_{\partial E} \mathbf{u}\cdot\mathbf{n} f_i \simeq \int_{\partial E} \mathbf{u}\cdot\mathbf{n} f_i^*.$$

Since f_i is constant in each element, we have

$$\int_E f_i \nabla\cdot\mathbf{u} = f_i|_E \int_E \nabla\cdot\mathbf{u} = f_i|_E \int_{\partial E} \mathbf{u}\cdot\mathbf{n}.$$

Consequently, we reach

$$\int_E \phi \frac{c^k\left(z_i^{k+1} - z_i^{k+1/2}\right)}{t_{k+1}-t_k} + \int_{\partial E} \mathbf{u}^{k+1}\cdot\mathbf{n} f_i^{k*} - f_i^k|_E \int_{\partial E} \mathbf{u}^{k+1}\cdot\mathbf{n} = 0,$$

which is used to explicitly compute the values of z_i^{k+1}.

Finally, the fugacities and mixture properties are calculated by using the Peng–Robinson equation of state [27].

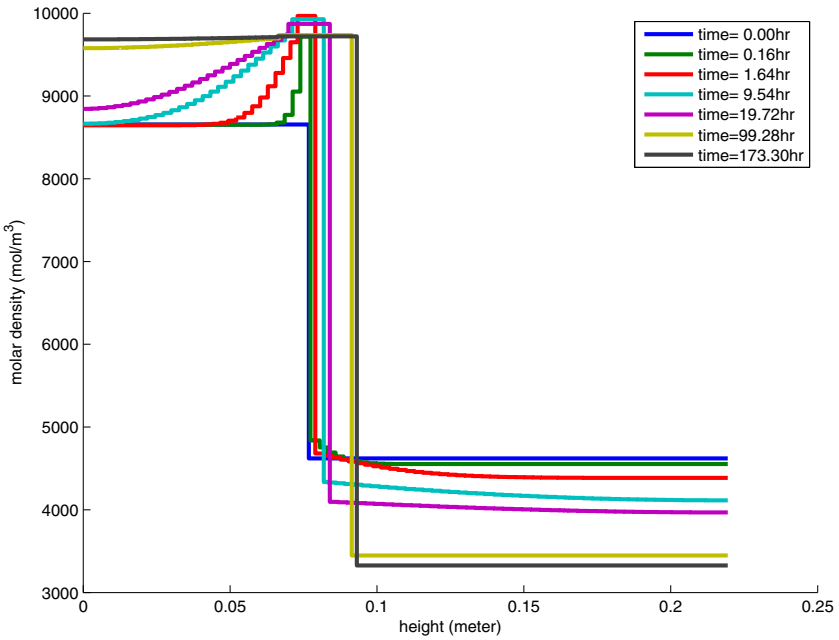

(a) Two-domain method

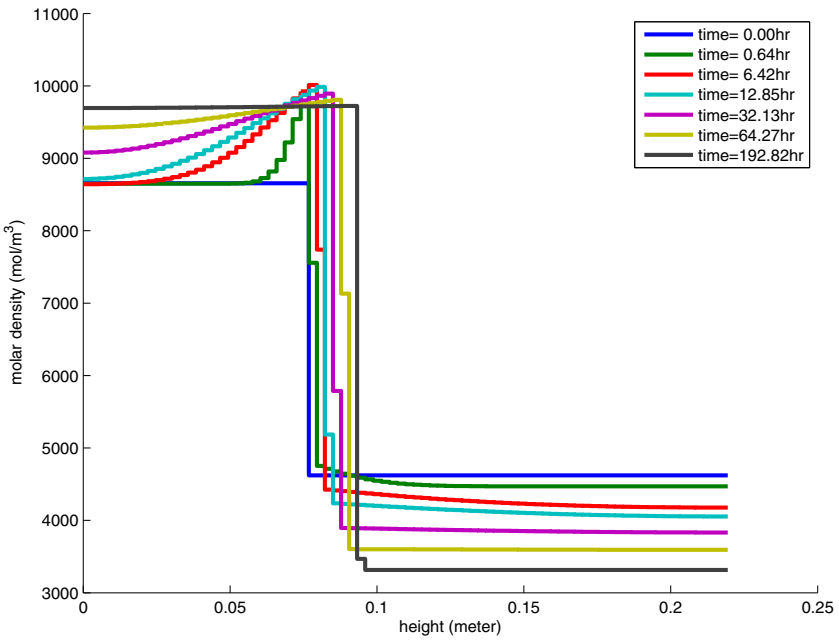

(b) Single-domain method

Fig. 5 Molar density simulated on a mesh of 80 cells

5 Numerical examples

5.1 1-D mixing dynamics: methane–pentane mixture

In this subsection, we simulate the mixing of methane–pentane mixture under the same condition as reported in [14]. One of the more comprehensive models of PVT cell experiments is tested on a methane–pentane mixture in [30]. The cell is initially saturated by pure components as vapor methane and liquid pentane. The evolution of pressure and liquid level for the same experiment has been simulated in [14] as a verification of their model. In this paper, we use the proposed numerical models to simulate the evolution of pressure, liquid level, composition, and molar density.

The PVT conditions are chosen to match those provided in [30]. The temperature (T) is constant both in the entire domain and with time. The height (H) of

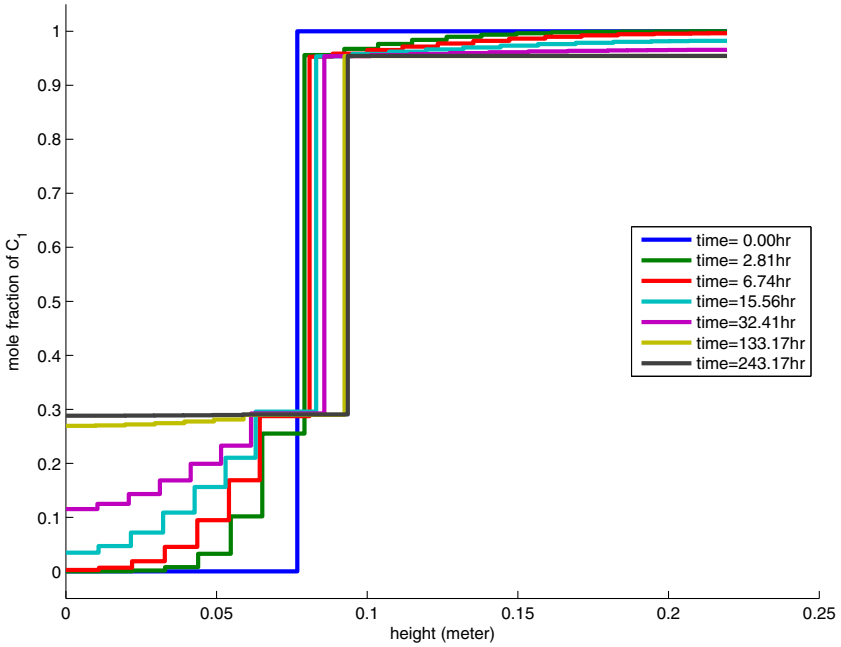

(a) Two-domain method

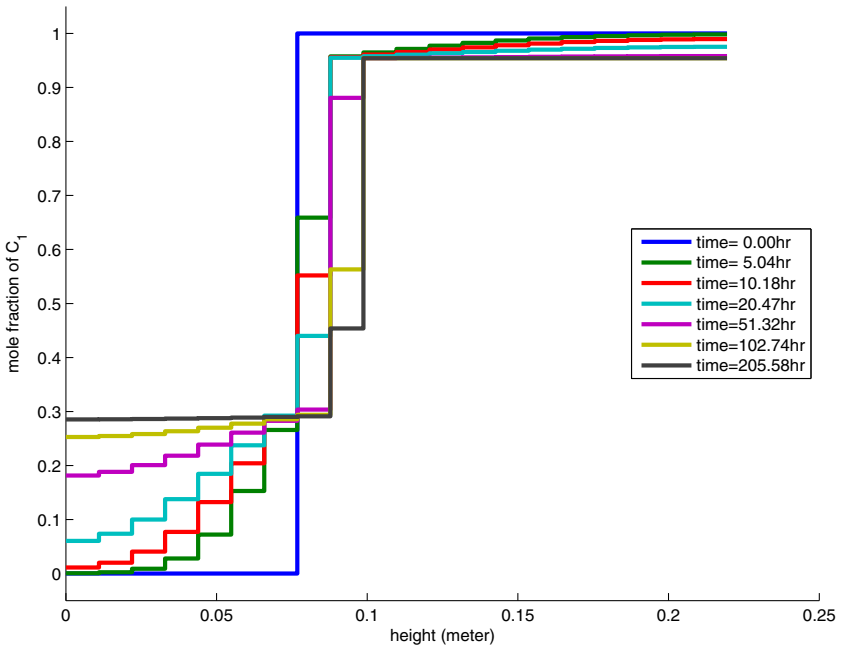

(b) Single-domain method

Fig. 6 Mole fraction of methane simulated on a mesh of 20 cells

the tested domain, and the initial values of liquid level (h_0) and pressure (P_0) are listed in Table 1. Provided in Table 2 are the component data used for calculating fugacity and mixture properties from the Peng–Robinson equation of state (PR-EOS) [27]. These input parameters for the PR-EOS include critical temperatures (T_c), critical pressures (P_c), and acentric factors (ω), which are from NIST Chemistry WebBook (http://webbook.nist.gov/chemistry). In addition, volume shift parameters (s) are from Jhaveri and Youngren [19]. When mixture properties are calculated, the binary interaction coefficient 0.054 is used in the PR-EOS. We use constant diffusion coefficients that are $D_L = 1.3 \times 10^{-8}$ m^2 s^{-1} and $D_G = 1.0 \times 10^{-7}$ m^2 s^{-1}, respectively [14].

For purpose of simplification, we use the explicit schemes for diffusion equations in the two methods proposed in this paper. In this case, the proposed methods suffer from the Courant number restriction

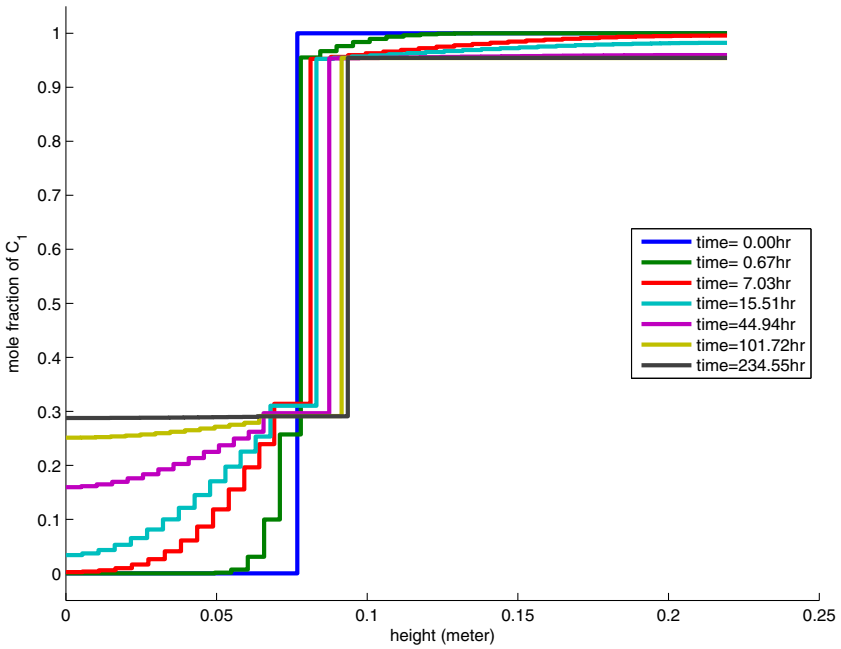

(a) Two-domain method

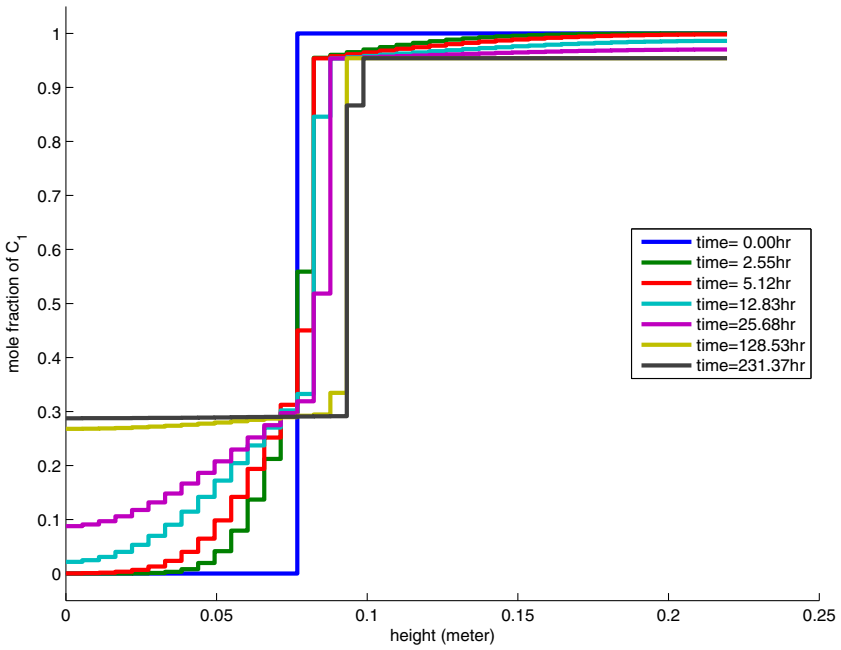

(b) Single-domain method

Fig. 7 Mole fraction of methane simulated on a mesh of 40 cells

on the time steps. As a result, the two-domain method needs to take very small time steps when the length of some elements becomes small, but the single-domain method can alleviate this restriction because of using fixed mesh. Therefore, the single-domain method can use much larger time step than the two-domain method (three or four times larger); the former is also more CPU efficient mainly due to allowed larger time step. In the future work, we will employ the implicit schemes for diffusion equations of the proposed numerical models to reduce Courant number restriction, and we will investigate the influence of this temporal treatment.

Figures 1 and 2 illustrate how the accuracy of simulated pressure drop and liquid level is influenced by the spatial mesh used for the two-domain and single-domain methods. The simulated results indicate that a mesh of ten (or more) grid cells can accurately simulate the pressure evolution, while a mesh of 20 (or

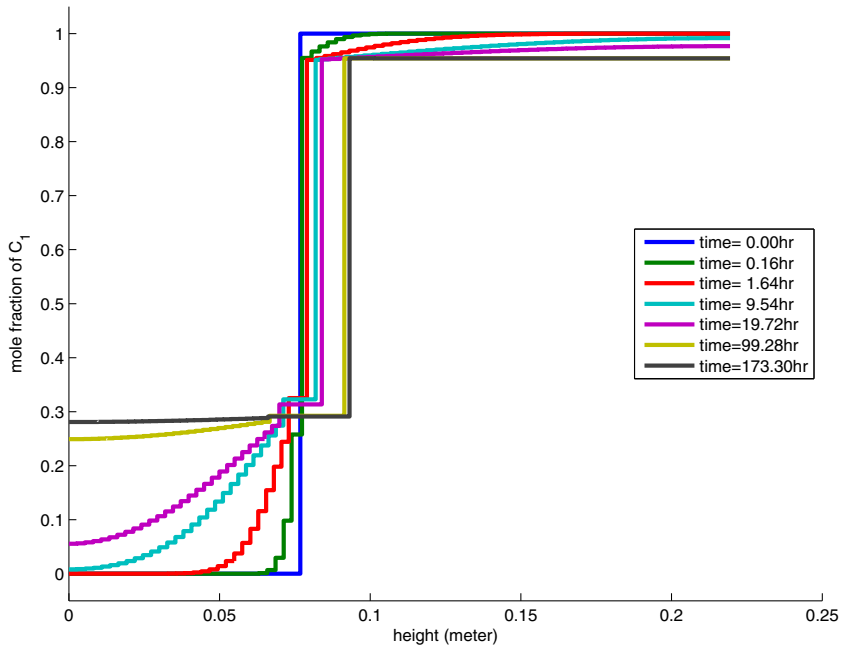

(a) Two-domain method

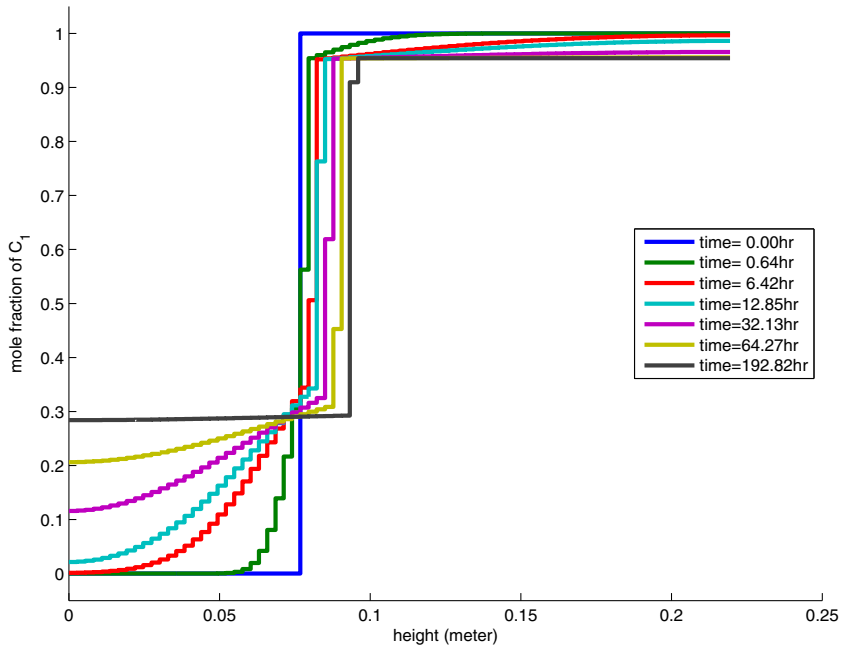

(b) Single-domain method

Fig. 8 Mole fraction of methane simulated on a mesh of 80 cells

more) grid cells accurately simulates the liquid level evolution, using either the two-domain or the single-domain method. On the other hand, a finer mesh is required for accurate resolution of the spatial profiles of quantities (such as molar density, mole fractions, saturations). With the same initial mesh, the single-domain method seems slightly less accurate than the two-domain method in predicting the evolution of the pressure and liquid level. This is probably because the single-domain method introduces more numerical diffusion in its solution (without capturing the saturation profile sharply or using much larger time steps).

Figures 3, 4, and 5 show molar density simulated by the two-domain and single-domain methods on different meshes. Figures 6, 7, and 8 show mole fraction of methane simulated by the two methods on different

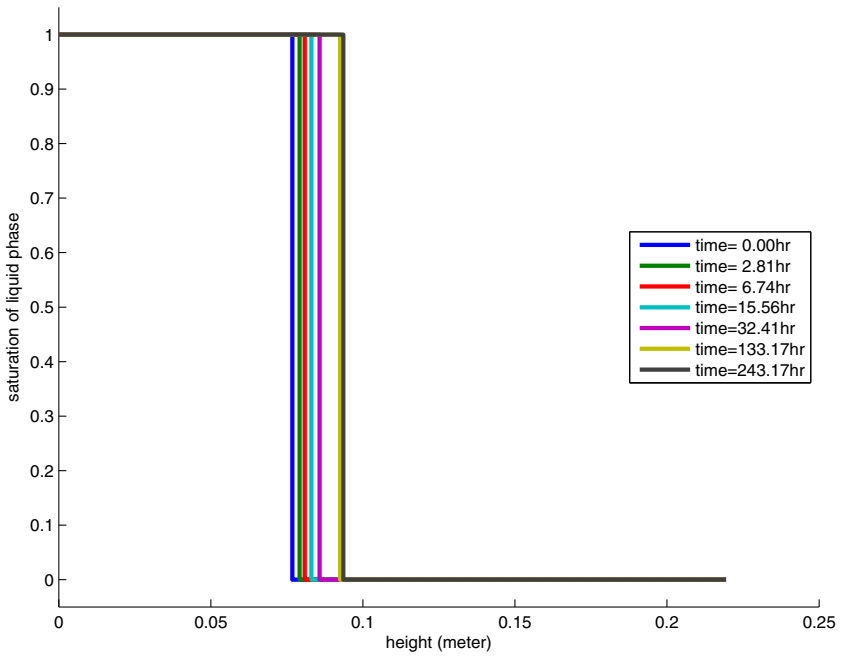

(a) Two-domain method

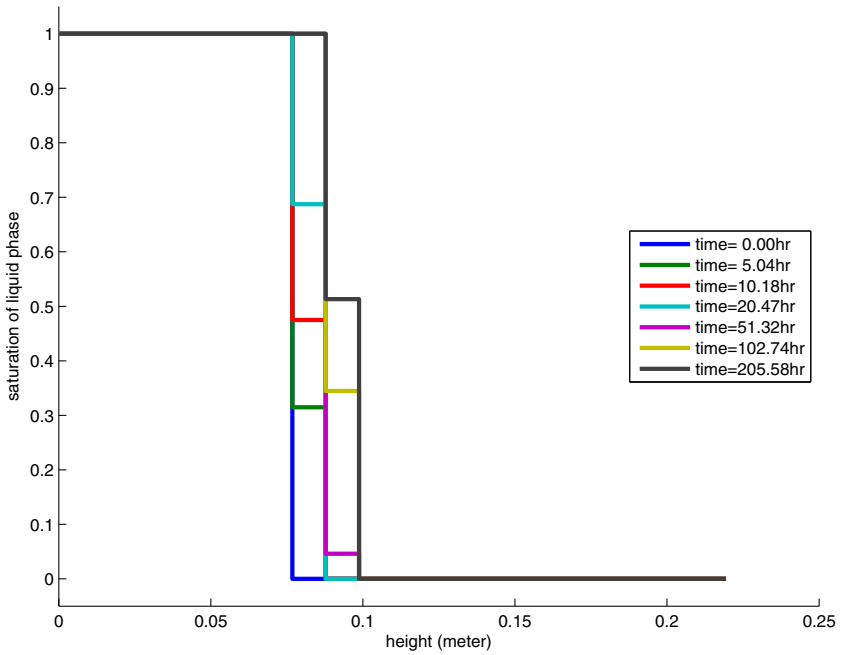

(b) Single-domain method

Fig. 9 Saturation of liquid phase simulated on a mesh of 20 cells

meshes. Molar density changes with the composition, which is determined by mass transfer occurring on the interface between two fluid phases by dissolution and evaporation, and in each fluid phase by the diffusion and convection. The processes occurring on the interface of two phases are generally much faster than the diffusive and convective time scales in either phase, and as a result, the overshoot of molar density happens around two-phase interface. For a binary system, the composition at the interface between two phases is uniquely determined by thermodynamic equilibrium; that is, interfacial composition depends only on temperature and pressure. In the problem, we keep the temperature constant. As shown in Figs. 6, 7, and 8, more gaseous methane dissolves in the liquid phase during the mixing process, and thus the pressure (constant in the entire domina) decreases with time, which is observed in Figs. 1 and 2.

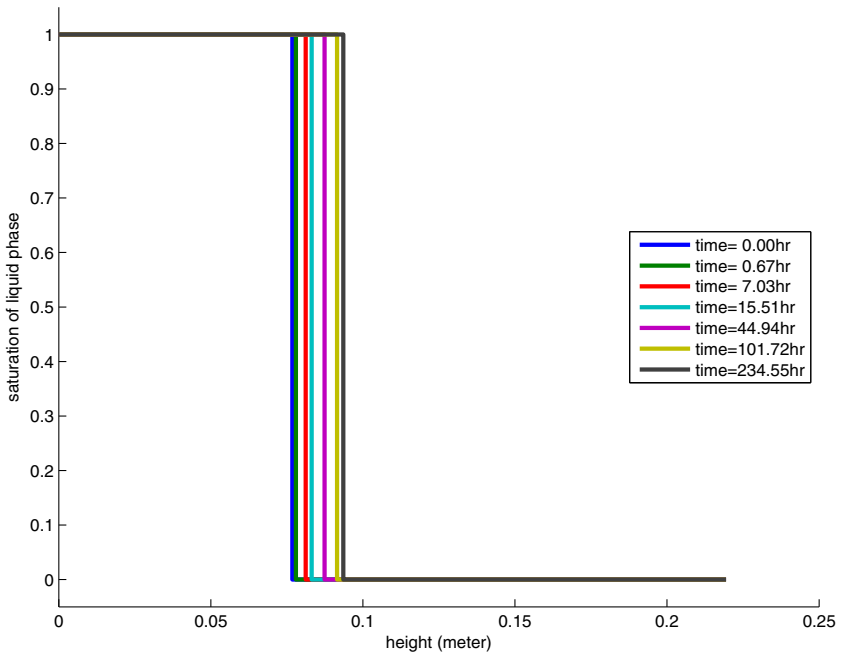

(a) Two-domain method

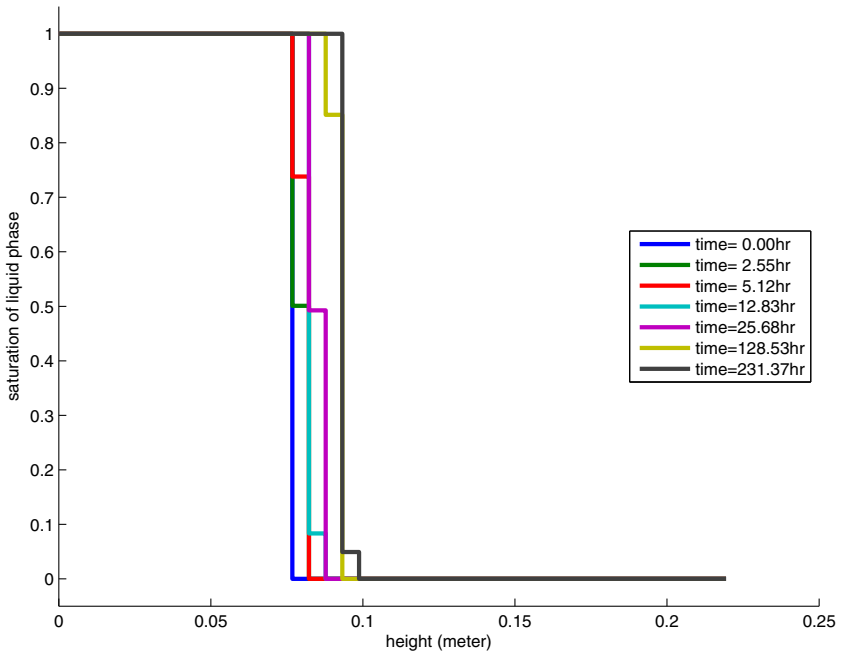

(b) Single-domain method

Fig. 10 Saturation of liquid phase simulated on a mesh of 40 cells

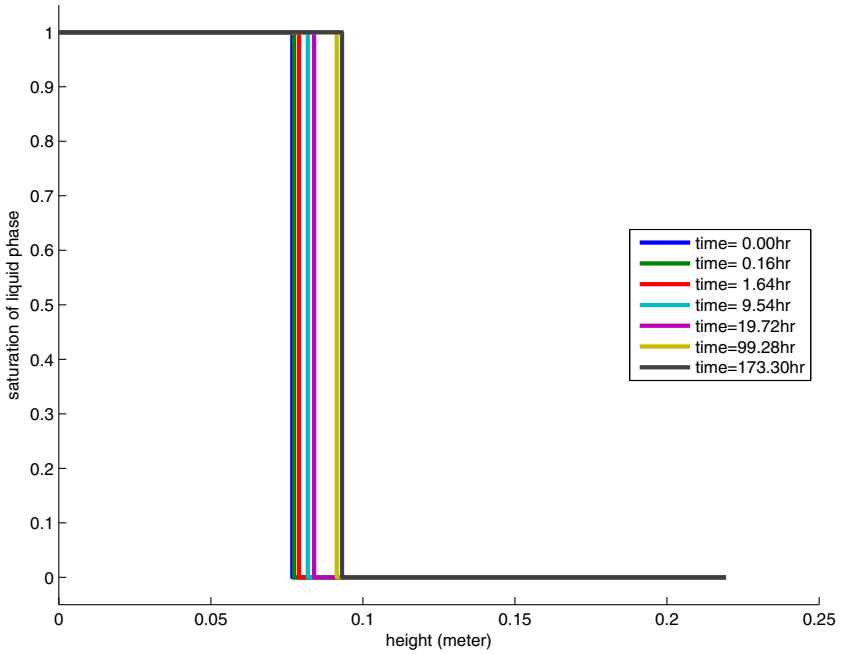

(a) Two-domain method

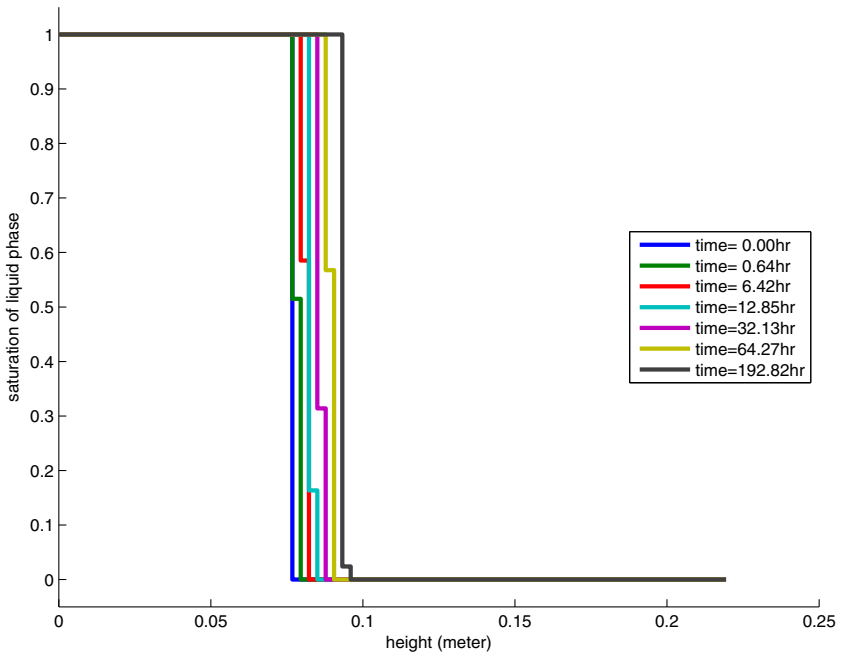

(b) Single-domain method

Fig. 11 Saturation of liquid phase simulated on a mesh of 80 cells

Figures 9, 10, and 11 show the saturation of liquid phase simulated by two methods on different meshes. The two-domain method produces saturation profiles with a sharp front, while the single-domain method introduces artificial two-phase region between the liquid-phase region and the gas-phase region. However, the artificial two-phase region is narrow (only a single element wide), and its width tends to decrease when using a finer mesh. Moreover, one can postprocess the result of saturation from the single-domain method to recover the sharp-jump saturation if needed.

Table 3 Component data used in the PR-EOS for 2-D experiment

	T_c (K)	P_c (MPa)	ω	s
CO_2	304.1	7.375	0.239	0.1137
nC_{10}	617.7	2.11	0.489	0.0865

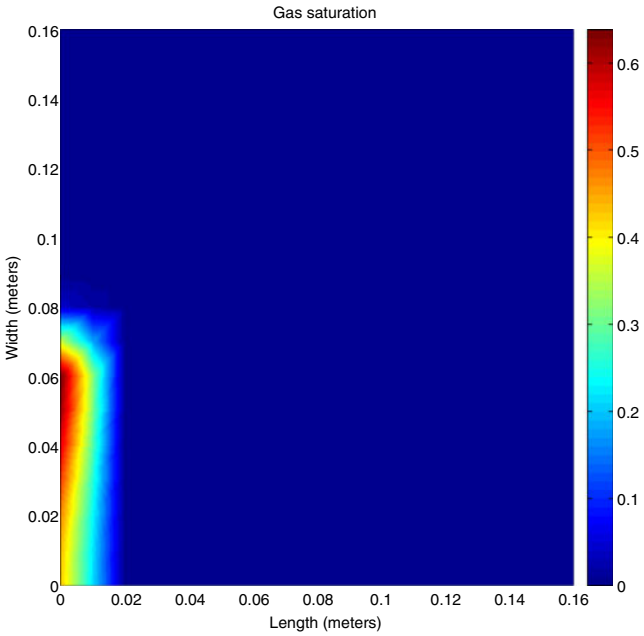

Fig. 12 Gas saturation at 5.0e+4 s

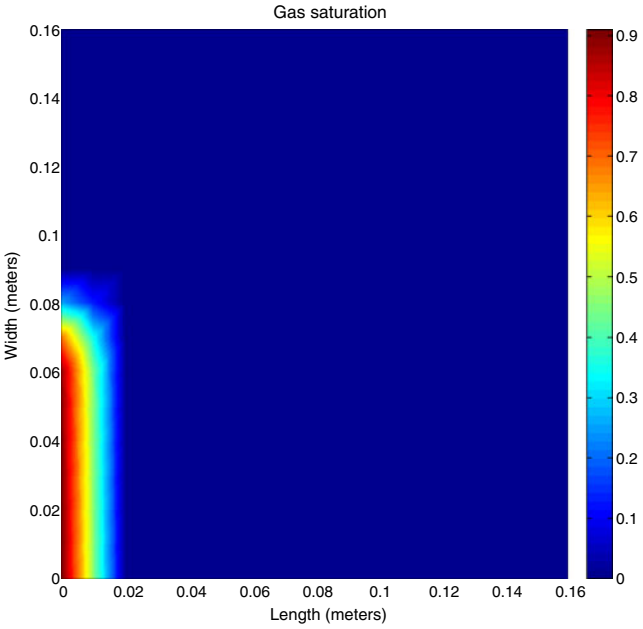

Fig. 14 Gas saturation at 5.0e+5 s

5.2 2-D displacement

In this example, we simulate the displacement of normal decane (nC_{10}) by carbon dioxide (CO_2) in a two-dimensional domain. The void space of the medium is initially fully saturated with nC_{10}, and then we flood the system by CO_2 on the lower half of the left boundary and produce outflow on the lower half of the right boundary. The other boundaries are impermeable. We use the proposed numerical models to simulate the evolution of mixture composition.

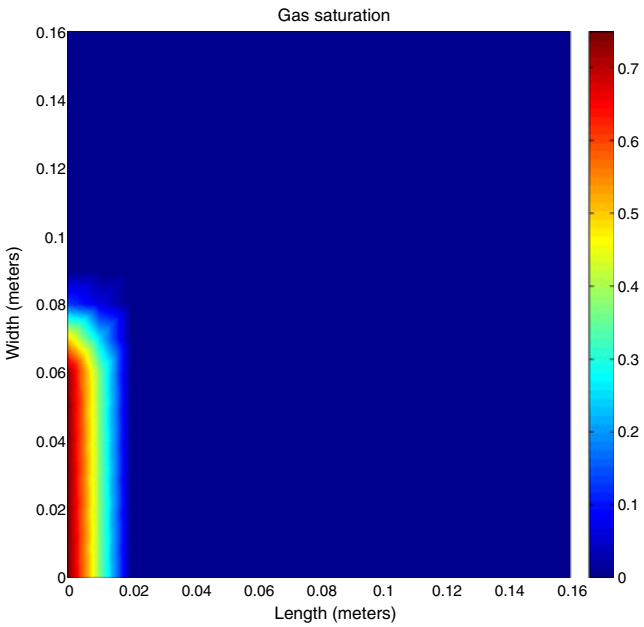

Fig. 13 Gas saturation at 2.0e+5 s

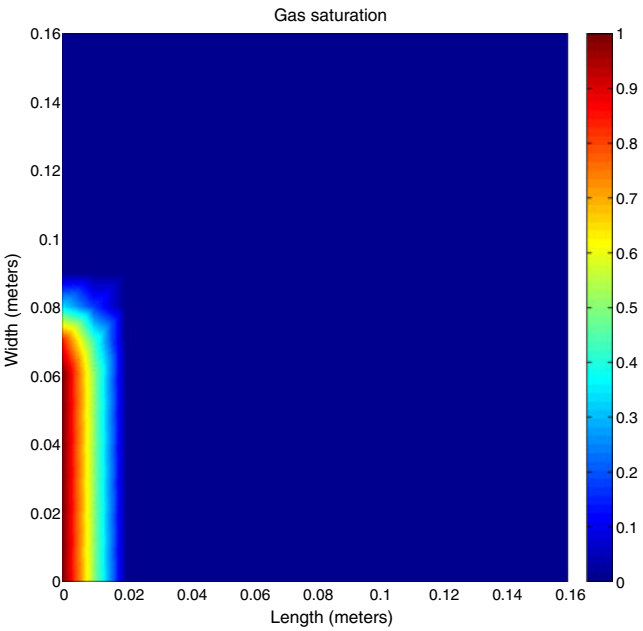

Fig. 15 Gas saturation at 8.3e+5 s

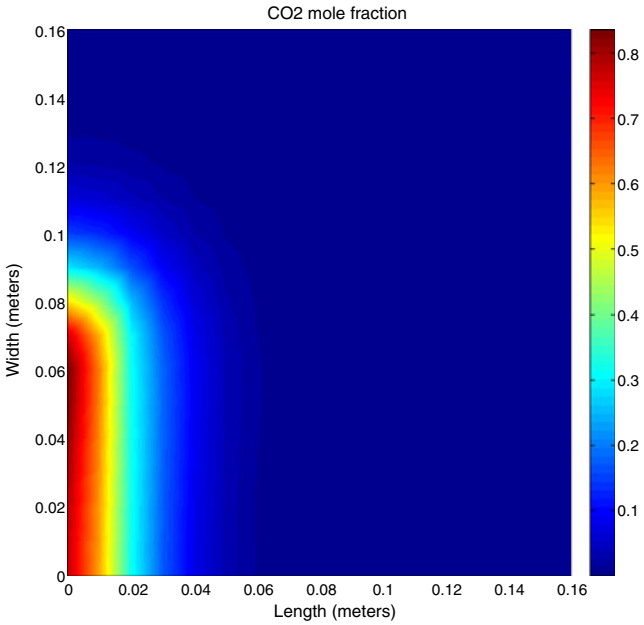

Fig. 16 CO_2 mole fraction at 5.0e+4 s

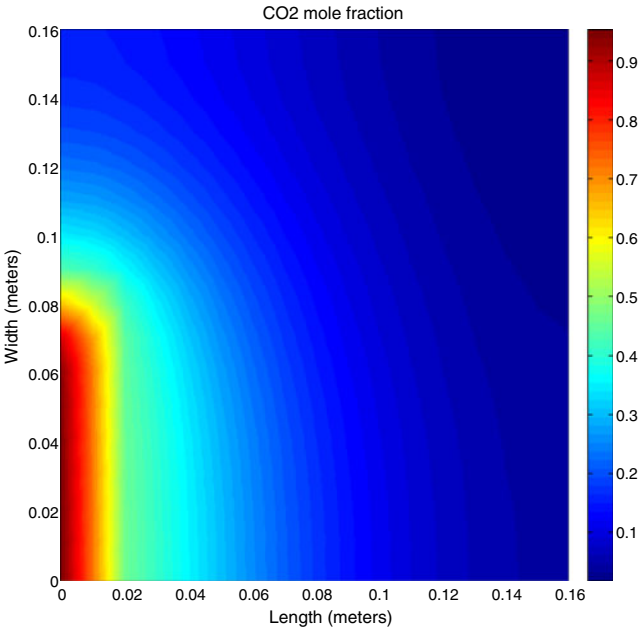

Fig. 18 CO_2 mole fraction at 5.0e+5 s

The domain is 0.16m × 0.16m × 1m. The temperature is 313.1 K, a constant over the entire domain and with time. The initial pressure is 4.01 MPa in the entire domain. Provided in Table 3 are the component data used for calculating fugacity and mixture properties from the PR-EOS. The data are chosen from those provided in [31]. The inflow and outflow velocities are $2e-7$ and $1.5e-7$ m/s. The effect of gravity is neglected. Diffusion coefficients are chosen to be constant: $D_G = 1.5e-7$ m^2/s and $D_L = 5.6e-9$ m^2/s. The domain is homogeneous with the permeability being 10^9 md. The viscosities of gas and liquid phases are 0.1 and

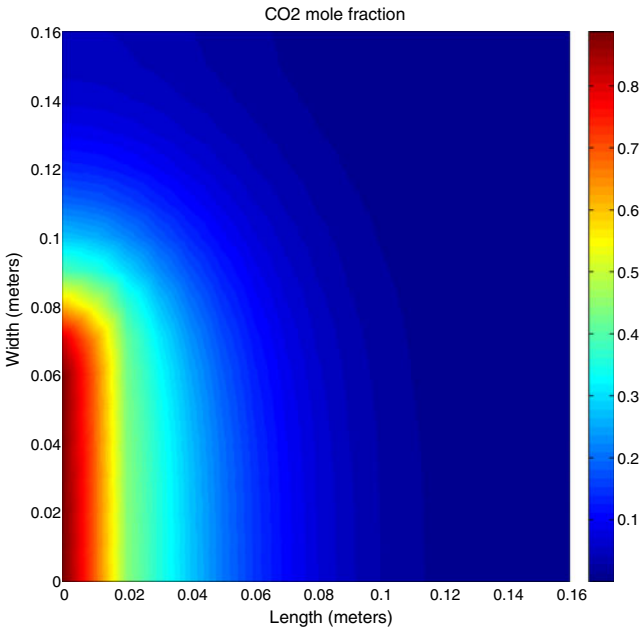

Fig. 17 CO_2 mole fraction at 2.0e+5 s

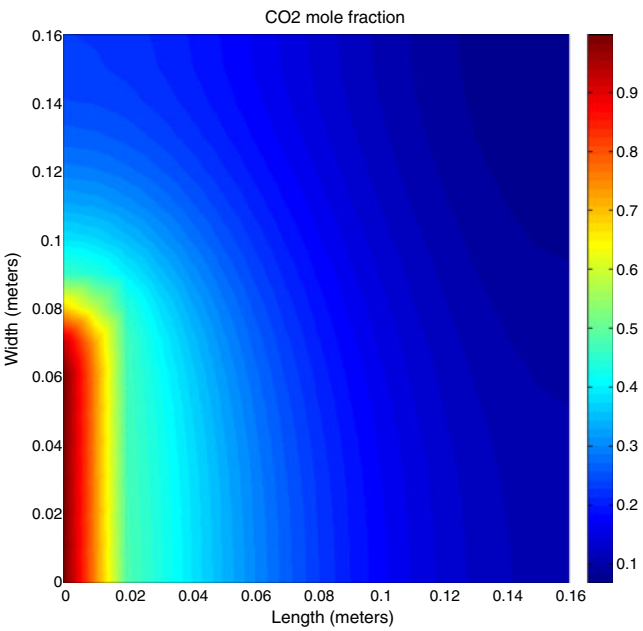

Fig. 19 CO_2 mole fraction at 8.3e+5 s

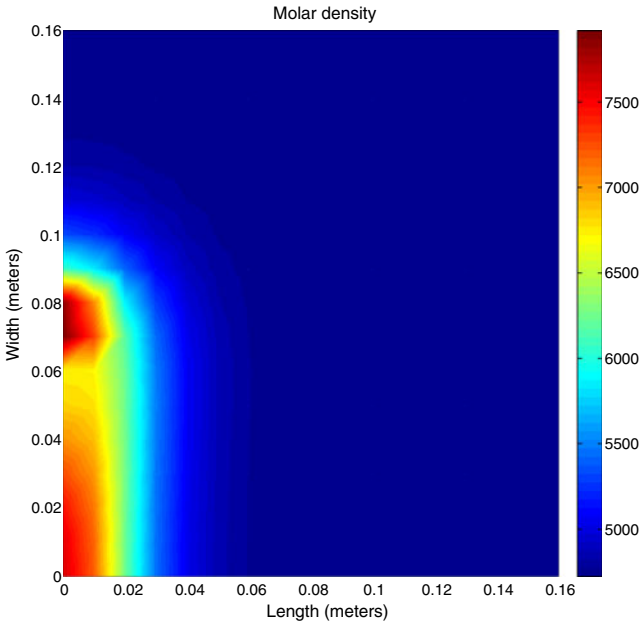

Fig. 20 Molar density at 5.0e+4 s

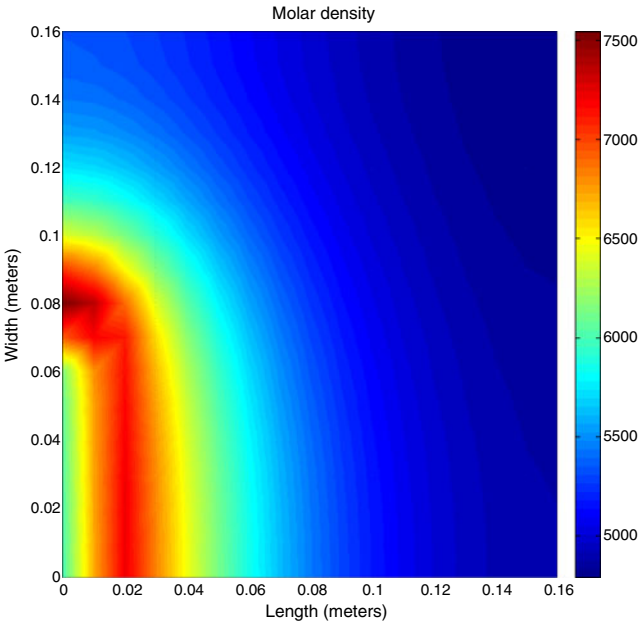

Fig. 22 Molar density at 5.0e+5 s

1.0 cp, respectively. The cubic relative permeability is employed.

An explicit scheme is used for convection and diffusion equations, and a small time step size of 100 s is used. We note that the pressure is almost constant in the entire domain at any given time (but varying with time) when the permeability is very large. Figures 12, 13, 14, and 15 show gas saturation profiles. Mole fraction of CO_2 and mixture molar density are shown in Figs. 16, 17, 18, and 19, and Figs. 20, 21, 22, and 23, respectively. Like the 1-D example, we also observe sharp moving fronts of saturation, mole fraction, and molar density simulated by the algorithm. The convection is dominated near the injection boundary, and the

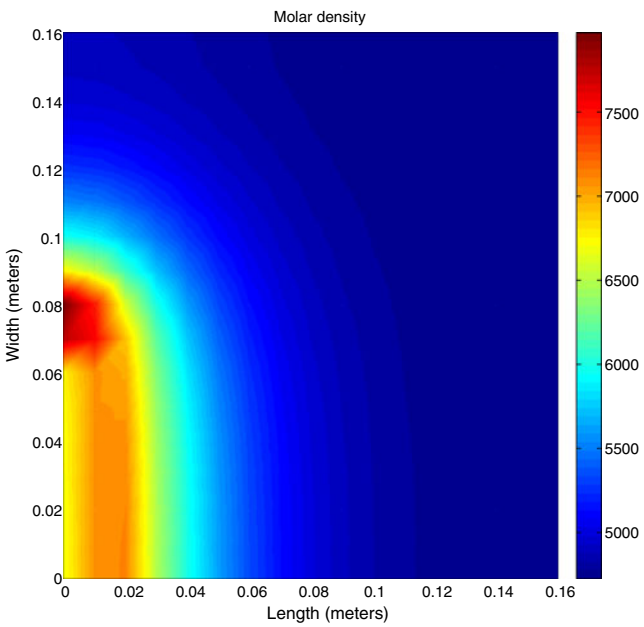

Fig. 21 Molar density at 2.0e+5 s

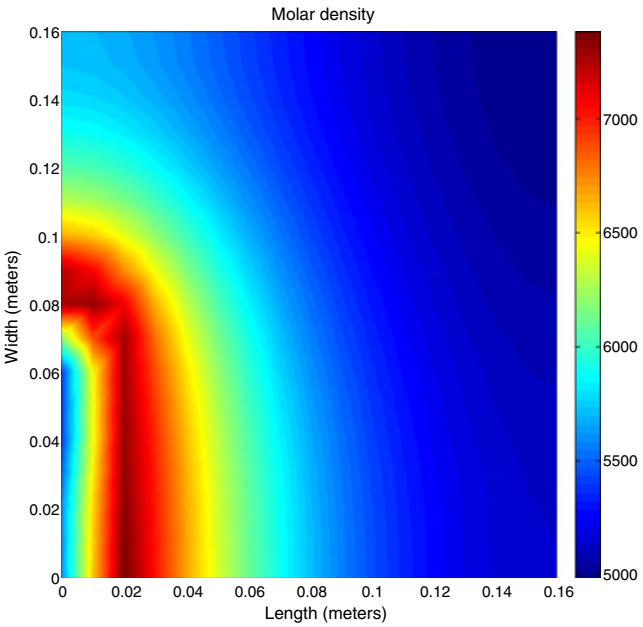

Fig. 23 Molar density at 8.3e+5 s

fluid composition changes not only with convection and diffusion but also with mass transfer occurring on the interface between two fluid phases.

6 Conclusions

We have developed a mathematical model for isothermal compositional two-phase flow in porous media. In each time step, we apply time splitting to decompose the original equation into two steps: diffusion step and convection step. Then we propose two deferent methods: single-domain and two-domain methods. In the two-domain method, based on the assumption that there exists a distinct interface between the liquid and gas phases, we divide the entire computational domain into two subdomains: the gas region and the liquid region, and then we use the characteristic finite element method with moving mesh to track the interface between two subdomains, which varies with time. We employ the mixed finite element method for diffusion equation. The single-domain method allows the saturation to vary between 0 and 1, and employs a fixed mesh. We derive the formulas to compute the diffusive flux for MFE. The single-domain method is extended to multiple dimensional domain.

Numerical results indicate that both two-domain and single-domain methods can accurately describe the evolution of the pressure and liquid level. We notice that with the same initial mesh, the single-domain method allows much larger time steps than the two-domain method, and is more efficient in CPU time.

Finally, we give a remark on the two methods proposed in this work. The two-domain method requires the mesh moving to capture the liquid–gas interface, while the single-domain method does not. In two or three spatial dimensional domains, it is difficult to capture the liquid–gas interface because of its complexity and irregularity. Therefore, the extension to multiple dimension is nontrivial for the two-domain method. In the two-domain method the refinement close to the interface is both complicated and CPU time intensive, but it is needed for this method. On the other hand, in the single-domain approach we do not need fine grids. All the grids can be the same size. In future, we will continue this effort and investigate the implicit schemes for diffusion equations.

Acknowledgements This work was supported by the member companies of the Reservoir Engineering Research Institute. Their support is greatly appreciated. The authors also cheerfully appreciate the generous support of the university research fund to the Computational Transport Phenomena Laboratory at KAUST. This work is partly support by Key Project of Chinese Ministry of Education (No.212109).

References

1. Abreu, E., Douglas, J., Furtado, F., Pereira, F.: Operator splitting for three-phase flow in heterogeneous porous media. Commun. Comput. Phys. **6**, 72–84 (2008)
2. Akrivis, G., Crouzeix, M., Makridakis, C.: Implicit-explicit multistep methods for quasilinear parabolic equations. Numer. Math. **82**(4), 521–541 (1999)
3. Ascher, U.M., Ruuth, S.J., Spiteri, R.J.: Implicit-explicit Runge-Kutta methods for time-dependent partial differential equations. Appl. Numer. Math. **25**(2–3), 151–167 (1997)
4. Chen, Z., Huan, G., Li, B.: An improved IMPES method for two-phase flow in porous media. Transp. Porous Media **54**(3), 361–376 (2004)
5. Chen, Z., Huan, G., Ma, Y.: Computational Methods for Multiphase Flows in Porous Media. Society for Industrial Mathematics (2006)
6. Coats, K.H.: IMPES stability: selection of stable timesteps. SPE J. **8**(2), 181–187 (2003)
7. Dawson, C., Sun, S., Wheeler, M.F.: Compatible algorithms for coupled flow and transport. Comput. Methods Appl. Mech. Eng. **193**(23–26), 2565–2580 (2004)
8. Dawson, C.N., Klíe, H., Wheeler, M.F., Woodward, C.S.: A parallel, implicit, cell-centered method for two-phase flow with a preconditioned Newton–Krylov solver. Comput. Geosci. **1**(3), 215–249 (1997)
9. Farago, I.: A modified iterated operator splitting method. Appl. Math. Model. **32**(8), 1542–1551 (2008)
10. Firoozabadi, A.: Thermodynamics of Hydrocarbon Reservoirs. McGraw-Hill Professional (1999)
11. Geiser, J.: Iterative operator-splitting methods with higher-order time integration methods and applications for parabolic partial differential equations. J. Comput. Appl. Math. **217**(1), 227–242 (2008)
12. Gjesdal, T.: Implicit-explicit methods based on strong stability preserving multistep time discretizations. Appl. Numer. Math. **57**(8), 911–919 (2007)
13. Haugen, K.B., Firoozabadi, A.: Composition at the interface between multicomponent nonequilibrium fluid phases. J. Chem. Phys. **130**, 064707 (2009)
14. Haugen, K.B., Firoozabadi, A.: Mixing of two binary nonequilibrium phases in one dimension. AIChE J. **55**(8), 1930–1936 (2009)
15. Hill, E.S., Lacey, W.N.: Rate of solution of propane in quiescent liquid hydrocarbons. Ind. Eng. Chem. **26**(12), 1327–1331 (1934)
16. Hoteit, H., Firoozabadi, A.: Numerical modeling of two-phase flow in heterogeneous permeable media with different capillarity pressures. Adv. Water Resour. **31**(1), 56–73 (2008)
17. Hundsdorfer, W., Ruuth, S.J.: IMEX extensions of linear multistep methods with general monotonicity and boundedness properties. J. Comput. Phys. **225**(2), 2016–2042 (2007)
18. Jamialahmadi, M., Emadi, M., Müller-Steinhagen, H.: Diffusion coefficients of methane in liquid hydrocarbons at high pressure and temperature. J. Pet. Sci. Eng. **53**(1–2), 47–60 (2006)
19. Jhaveri, B., Youngren, G.: Three-parameter modification of the Peng-Robinson equation of state to improve volumetric predictions. SPE Reserv. Eng. **3**(3), 1033–1040 (1988)
20. Kanney, J.F., Miller, C.T., Kelley, C.T.: Convergence of iterative split-operator approaches for approximating nonlinear

reactive transport problems. Adv. Water Resour. **26**(3), 247–261 (2003)
21. Koto, T.: Stability of IMEX Runge-Kutta methods for delay differential equations. J. Comput. Appl. Math. **211**(2), 201–212 (2008)
22. Kou, J., Sun, S.: A new treatment of capillarity to improve the stability of IMPES two-phase flow formulation. Comput. Fluids **39**(10), 1293–1931 (2010)
23. Kou, J., Sun, S.: On iterative IMPES formulation for two phase flow with capillarity in heterogeneous porous media. Int. J. Numer. Anal. Model. Series B **1**(1), 20–40 (2010)
24. Lanser, D., Verwer, J.G.: Analysis of operator splitting for advection-diffusion-reaction problems from air pollution modelling. J. Comput. Appl. Math. **111**(1–2), 201–216 (1999)
25. Lohrenz, J., Bray, B., Clark, C.: Calculating viscosities of reservoir fluids from their compositions. J. Pet. Technol. **16**(10), 1171–1176 (1964)
26. Mikyska, J., Firoozabadi, A.: Implementation of higher-order methods for robust and efficient compositional simulation. J. Comput. Phys. **229**(8), 2898–2913 (2010)
27. Peng, D.-Y., Robinson, D.B.: A new two-constant equation of state. Ind. Eng. Chem. Fundam. **15**(1), 59–64 (1976)
28. Pomeroy, R.D., Lacey, W.N., Scudder, N.F., Stapp, F.P.: Rate of solution of methane in quiescent liquid hydrocarbons. Ind. Eng. Chem. **25**(9), 1014–1019 (1933)
29. Reamer, H.H., Opfell, J.B., Sage, B.H.: Diffusion coefficients in hydrocarbon systems methane-decane-methane in liquid phase-methane-decane-methane in liquid phase. Ind. Eng. Chem. **48**(2), 275–282 (1956)
30. Riazi, M.R.: A new method for experimental measurement of diffusion coefficients in reservoir fluids. J. Pet. Sci. Eng. **14**(3–4), 235–250 (1996)
31. Rongy, L., Haugen, K.B., Firoozabadi, A.: Mixing from fickian diffusion and natural convection in binary non-equilibrium fluid phases. AIChE J. **58**(5), 1336–1345 (2012)
32. Sun, S., Geiser, J.: Multiscale discontinuous Galerkin and operator-splitting methods for modeling subsurface flow and transport. Int. J. Multiscale Com. **6**(1), 87–101 (2008)
33. Sun, S., Wheeler, M.F.: A posteriori error estimation and dynamic adaptivity for symmetric discontinuous Galerkin approximations of reactive transport problems. Comput. Methods Appl. Mech. Eng. **195**(7–8), 632–652 (2006)
34. Sun, S., Wheeler, M.F.: Anisotropic and dynamic mesh adaptation for discontinuous Galerkin methods applied to reactive transport. Comput. Methods Appl. Mech. Eng. **195**(25–28), 3382–3405 (2006)
35. Tharanivasan, A.K., Yang, C., Gu, Y.: Measurements of molecular diffusion coefficients of carbon dioxide, methane, and propane in heavy oil under reservoir conditions. Energy Fuels **20**(6), 2509–2517 (2006)
36. Upreti, S.R., Mehrotra, A.K.: Experimental measurement of gas diffusivity in bitumen: results for carbon dioxide. Ind. Eng. Chem. Res. **39**(4), 1080–1087 (2000)
37. Watts, J.W.: A compositional formulation of the pressure and saturation equations. SPE Reserv. Eng. **1**(3), 243–252 (1986)
38. Young, L., Stephenson, R.: A generalized compositional approach for reservoir simulation. Old Soc. Pet. Eng. J. **23**(5), 727–742 (1983)